Front. Phys.
https://doi.org/10.15302/frontphys.2026.086301
CN 11-5994/O4
ISSN 2095-0462

REVIEW ARTICLE

# Laser-induced breakdown spectroscopy in China over the past decade: A first-principles and problem-oriented review

Shu Chen[1], Weilun Gu[4], Zongyu Hou[1], Yihan Lyu[1], Hongbin Ding[5], Lanxiang Sun[6], Ye Tian[7], Qianqian Wang[8], Lianbo Guo[9], Lei Zhang[10], Shunchun Yao[11], Duixiong Sun[12], Zhe Wang[1,2,3,‡]

[1]State Key Laboratory of Power System Operation and Control, International Joint Laboratory on Low Carbon Clean Energy Innovation, Department of Energy and Power Engineering, Tsinghua University, Beijing 100084, China

[2]Shanxi Research Institute for Clean Energy, Tsinghua University, Shanxi 030032, China

[3]School of Energy and Electrical Engineering, Qinghai University, Key Laboratory of Intelligent Operation of New Energy Power System of Ministry of Education, Xining 810016, China

[4]School of Integrated Circuits, Jiangnan University, Wuxi 214122, China

[5]School of Physics, Dalian University of Technology, Dalian 116024, China

[6]State Key Laboratory of Robotics and Intelligent Systems, Shenyang Institute of Automation, Chinese Academy of Sciences, Shenyang 110016, China

[7]College of Physics and Optoelectronic Engineering, Ocean University of China, Qingdao 266100, China

[8]School of Optics and Photonics, Beijing Institute of Technology, Beijing 100081, China

[9]Wuhan National Laboratory for Optoelectronics (WNLO), Huazhong University of Science and Technology, Wuhan 430074, China

[10]State Key Laboratory of Quantum Optics and Optics Devices, Institute of Laser Spectroscopy, Shanxi University, Taiyuan 030004, China

[11]School of Electric Power Engineering, South China University of Technology, Guangzhou 510640, China

[12]Key Laboratory of Atomic and Molecular Physics & Functional Materials of Gansu Province, College of Physics and Electronic Engineering, Northwest Normal University, Lanzhou 730070, China

Received April 14, 2026; accepted May 23, 2026

## Abstract

Owing to its inherent advantages, such as minimal sample preparation, real-time and simultaneous multi-element detection, and outstanding potential for in-situ and online analysis, laser-induced breakdown spectroscopy (LIBS) has become one of the indispensable spectroscopic techniques for elemental analysis and has greatly advanced elemental analysis in critical fields such as industrial quality control, geological exploration, aerospace detection, and fusion energy research. Over the past decade, LIBS research in China has achieved remarkable and comprehensive progress, making it timely to re-examine the current status of the field and identify the key directions that require further intensive investigation. For the first time, this review adopts a problem-oriented perspective to identify the key problems and summarize recent progress, anchored in the first principle of LIBS, as clarified in recent years: the essence of LIBS lies in the fact that its signal source is a highly transient and spatially inhomogeneous laser-induced plasma, which distinguishes it from other spectroscopic techniques. Based on this understanding, three core problems spanning the entire LIBS analytical chain are identified as the framework of this review: the generation of repeatable and stable signals through the formation of a more stable and repeatable plasma; the transformation of raw signals into reliable analytical results through the reduction of matrix effects and signal

uncertainty; and the maintenance of reliable analytical performance under practical deployment constraints. Under this framework, this paper reviews the latest research progress in LIBS in China from four aspects: fundamental plasma physics research, instrumental innovation and integration, data processing and modeling methodologies, and representative practical applications. It is shown that Chinese LIBS research has evolved from isolated methodological improvements to a more integrated research paradigm that synergistically combines plasma physics, signal acquisition, analytical modeling, and scenario-specific implementation. Despite these significant advances, critical challenges remain, including refined and predictive plasma modeling, systematic characterization of coupled signal-formation effects, enhanced robustness and transferability of analytical models, and the maintenance of reliable analytical performance under real deployment scenarios. Future development of LIBS in China is expected to rely on the interdisciplinary integration and joint advancement of deeper physical understanding of laser-induced plasma, more generalizable analytical methodologies, and more sophisticated engineering implementation for practical deployment.

**Keywords** laser-induced breakdown spectroscopy, LIBS, laser-induced plasma, plasma modulation, quantitative analysis, industrial application



## Just Accepted

# Laser-Induced Breakdown Spectroscopy in China Over the Past Decade: A First-Principles and Problem-Oriented Review

Shu Chen[1], Weilun Gu[4], Zongyu Hou[1], Yihan Lyu[1], Hongbin Ding[5], Lanxiang Sun[6], Ye Tian[7], Qianqian Wang[8], Lianbo Guo[9], Lei Zhang[10], Shunchun Yao[11], Duixiong Sun[12], and Zhe Wang*[1,2,3]

[1]State Key Laboratory of Power System Operation and Control, International Joint Laboratory on Low Carbon Clean Energy Innovation, Department of Energy and Power Engineering, Tsinghua University, Beijing 100084, China
[2]Shanxi Research Institute for Clean Energy, Tsinghua University, Shanxi 030032, China
[3]School of Energy and Electrical Engineering, Qinghai University, Key Laboratory of Intelligent Operation of New Energy Power System of Ministry of Education, Xining 810016, China
[4]School of Integrated Circuits, Jiangnan University, Wuxi 214122, China
[5]School of Physics, Dalian University of Technology, Dalian 116024, China
[6]State Key Laboratory of Robotics and Intelligent Systems, Shenyang Institute of Automation, Chinese Academy of Sciences, Shenyang 110016, China
[7]College of Physics and Optoelectronic Engineering, Ocean University of China, Qingdao 266100, China
[8]School of Optics and Photonics, Beijing Institute of Technology, Beijing 100081, China
[9]Wuhan National Laboratory for Optoelectronics (WNLO), Huazhong University of Science and Technology, Wuhan 430074, China
[10]State Key Laboratory of Quantum Optics and Optics Devices, Institute of Laser Spectroscopy, Shanxi University, Taiyuan 030004, China
[11]School of Electric Power Engineering, South China University of Technology, Guangzhou 510640, China
[12]Key Laboratory of Atomic and Molecular Physics & Functional Materials of Gansu Province, College of Physics and Electronic Engineering, Northwest Normal University, Lanzhou 730070, China

May 23, 2026

**Abstract**

Owing to its inherent advantages, such as minimal sample preparation, real-time and simultaneous multi-element detection, and outstanding potential for in-situ and online analysis, laser-induced breakdown spectroscopy (LIBS) has become one of the indispensable spectroscopic techniques for elemental analysis and has greatly advanced elemental analysis in critical fields such as industrial quality control, geological exploration, aerospace detection, and fusion energy research. Over the

*Corresponding author. Email: zhewang@tsinghua.edu.cn

past decade, LIBS research in China has achieved remarkable and comprehensive progress, making it timely to re-examine the current status of the field and identify the key directions that require further intensive investigation. For the first time, this review adopts a problem-oriented perspective to identify the key problems and summarize recent progress, anchored in the first principle of LIBS, as clarified in recent years: the essence of LIBS lies in the fact that its signal source is a highly transient and spatially inhomogeneous laser-induced plasma, which distinguishes it from other spectroscopic techniques. Based on this understanding, three core problems spanning the entire LIBS analytical chain are identified as the framework of this review: the generation of repeatable and stable signals through the formation of a more stable and repeatable plasma; the transformation of raw signals into reliable analytical results through the reduction of matrix effects and signal uncertainty; and the maintenance of reliable analytical performance under practical deployment constraints. Under this framework, this paper reviews the latest research progress in LIBS in China from four aspects: fundamental plasma physics research, instrumental innovation and integration, data processing and modeling methodologies, and representative practical applications. It is shown that Chinese LIBS research has evolved from isolated methodological improvements to a more integrated research paradigm that synergistically combines plasma physics, signal acquisition, analytical modeling, and scenario-specific implementation. Despite these significant advances, critical challenges remain, including refined and predictive plasma modeling, systematic characterization of coupled signal-formation effects, enhanced robustness and transferability of analytical models, and the maintenance of reliable analytical performance under real deployment scenarios. Future development of LIBS in China is expected to rely on the interdisciplinary integration and joint advancement of deeper physical understanding of laser-induced plasma, more generalizable analytical methodologies, and more sophisticated engineering implementation for practical deployment.

**Keywords:** laser-induced breakdown spectroscopy; LIBS; laser-induced plasma; plasma modulation; quantitative analysis; industrial application

# 1 Introduction

As one of the most promising analytical technologies, laser-induced breakdown spectroscopy (LIBS) has attracted extensive attention over the past years owing to its minimal sample preparation, rapid response, multi-element detection capability, and potential for in-situ or online analysis. In 2014, a review article was published to summarize the progress of LIBS research in China and discuss the associated challenges and opportunities for future development [1], marking the beginning of a period of rapid growth in Chinese LIBS research. Since then, extensive research from China has been conducted and published as shown in Fig. 1, contributing to a prosperous decade of LIBS together with the growth of the Chinese and Asian LIBS community [2–7]. Therefore, it is timely to provide a reassessment.

This review aims to summarize the development of LIBS research in China over the past decade, as well as to discuss the remaining unsolved key problems and future directions. As an updated review, its main structure remains the same as that of the previous one [1], including fundamentals, instrumentation, data processing and modeling, and applications. In particular, this review places special emphasis on LIBS quantification, as quantitative capability remains the Achilles' heel of LIBS. Moreover, a dedicated section,

Section 2, is included to highlight and discuss the key problems in LIBS quantification and industrial application.

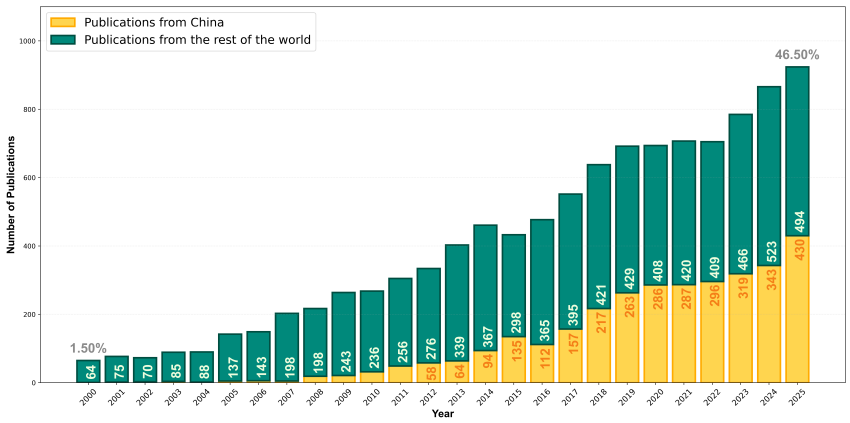


Figure 1: Annual number of LIBS publications worldwide and in China (2000-2025), retrieved from Web of Science All Databases.

# 2 Discussion of Insights

As Albert Einstein said, "The formulation of a problem is often more essential than its solution," [8] the authors realized that, when facing the critical challenges of LIBS quantification and the tremendous amount of work conducted or still to be conducted, it would be more enlightening and conclusive from a problem-oriented point of view. Therefore, in the present work, we organize recent developments within a problem-oriented framework of core problems, key problems, and sub-key problems, and discuss possible directions for future investigations on this basis.

Such a problem-oriented framework should first be rooted in the essential nature of LIBS itself. It was recently clarified that, compared with other traditional spectroscopic techniques such as Raman and X-ray fluorescence (XRF), the essential difference of LIBS lies in the fact that its signal source is a highly transient and spatially inhomogeneous plasma [9]. Therefore, from a first-principles perspective, the research methods and technical routes for LIBS quantitative analysis can be more systematically organized around this essence. It should be clarified that, in this review, the term "first principles" is not intended to imply an approach in which the entire LIBS process and the resulting signal are completely derived from fundamental physical laws, nor that this derivation is practically achievable. Rather, the term is used in a more conceptual and perspective-oriented sense. It refers to taking the essential characteristic that distinguishes LIBS from other spectroscopic techniques as the starting point, adopting a plasma-centered way of thinking. In this sense, we regard this essence as the first principle of LIBS in this review. From this perspective, to improve LIBS analytical performance and industrial application, the most critical issue is to produce a much more repeatable laser-induced plasma (LIP) or cancel out the effects caused by its drastic spatiotemporal variation. For example, as shown in Fig. 2, with this essence as the first principle, the research methodology of LIBS should shift to an understanding centered on plasma evolution, which serves as the bridge between experimental parameters and observable signals, rather than directly studying the impact of different parameters on signals. Based on this plasma-centered perspective,

the entire LIBS analytical process can be divided into three stages: plasma evolution and signal acquisition, data processing, and practical application. The two well-known bottlenecks in LIBS analysis, namely signal uncertainty and matrix effects, can also be viewed along this analytical chain. In this chain, upstream disturbances may be propagated to downstream stages, while each stage may also introduce additional sources of fluctuations or bias. Both signal uncertainty and matrix effects should therefore be regarded as issues that need to be addressed at each stage.

In the stage of plasma evolution and signal acquisition, fluctuations in plasma morphology, temperature, electron density, and species distribution are manifested as fluctuations in spectral-line intensity and continuum background. These plasma fluctuations may also affect the line profile in two ways: by changing spectral-line broadening through various broadening mechanisms, and by changing the population of relevant energy levels and the spatial distribution of emitting and absorbing species, thereby altering the degree of self-absorption. This transmission from plasma fluctuations to signal uncertainty is strongly affected by the spatiotemporal acquisition window, because the acquired spectrum is basically a projection of plasma evolution within a selected spatial and temporal range. Therefore, the core problem of this stage is: How to obtain signals with better repeatability and reduced matrix effects? This problem involves several closely related aspects, including the desirable plasma evolution process for reducing signal uncertainty and matrix effects, the mechanisms of laser–sample interaction and plasma–surrounding gas interaction leading to this desirable evolution, and the optimization of the spatiotemporal signal-collection window.

In the data-processing stage, the fluctuations and distortions contained in the raw spectra need to be properly corrected, compensated, or represented. Otherwise, they may be transformed into excessive feature shifts, calibration bias and prediction uncertainty. Therefore, the core problem of this stage is: How to transform raw signals into reliable analytical results? This problem involves the impacts of matrix effects and signal fluctuations on analytical results, and the principles for reducing, correcting or compensating for them.

In practical deployment, on the one hand, factors such as instrument drift, matrix drift and environmental disturbances introduce additional sources of uncertainty for the plasma-centered process. On the other hand, the practical constraints may sometimes reshape the entire analytical chain. For example, underwater LIBS must operate in a high-pressure liquid environment, which strongly changes plasma formation, plasma evolution, signal acquisition, and subsequent modeling. The third core problem is: How to maintain reliable analytical performance under practical constraints? This problem involves long-term stability and robustness, transferability and adaptation among different setups or scenarios, model self-adaptation and continual learning in online measurements, adaptation under limited real-world data, and scenario-oriented deployment.

For clarity, the above problems, together with the sub-key problems derived from them, are listed in Table 1. It should be noted that, in order to distinguish the roles of signal uncertainty and matrix effects, signal uncertainty should be addressed first, because sufficiently repeatable signals provide the basis for identifying, representing, or compensating for matrix effects. Matrix effects, in turn, should be understood from a plasma-centered perspective rather than a merely laser-sample-interaction view. This will be discussed in detail in Section 3.1.1. In addition, this problem-oriented framework also implies a corresponding logic for evaluating LIBS methods and models. Enhancement factors (EF), signal-to-noise ratio (SNR), signal-to-background ratio (SBR), limit of

detection (LOD), relative standard deviation (RSD), and classification accuracy should not themselves be regarded as complete evidence of improved quantitative reliability. Improved analytical capability should ultimately be supported by downstream evidence, such as consistently reduced prediction error, improved external validation performance, reduced prediction uncertainty, and better robustness across different matrices or instruments. For practical deployment, evaluation should further consider long-term stability, tolerance to instrumental and environmental drift, transferability, adaptation under limited real-world data, and performance on representative practical samples, according to the specific needs and constraints. Therefore, the evaluation criteria should be selected according to the analytical objective, method type, and application scenario, and intermediate indicators should be interpreted as supporting evidence rather than direct proof of improved quantitative capability. Nevertheless, some intermediate indicators are useful at the level of problem decomposition. For instance, an improvement in the RSD of the original signal usually contributes to the reproducibility of quantitative results.

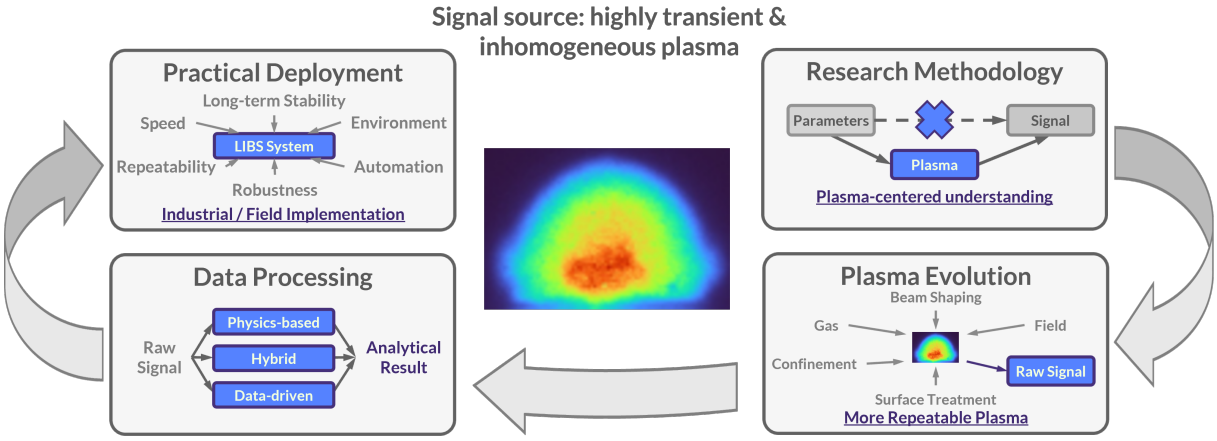


Figure 2: Research orientation framework for LIBS based on first-principle thinking.

Table 1: Problem-oriented framework of LIBS: core, key, and sub-key problems.

| Main Process | Core Problem | Key Problems | Sub-Key Problems |
|---|---|---|---|
| Plasma formation, evolution, and signal acquisition | How to obtain signals with better repeatability and reduced matrix effects? | What is the desirable plasma evolution process for reducing signal uncertainty and matrix effects? | What is the correlation among matrix effects, signal uncertainty, and plasma evolution, and what are the corresponding reduction mechanisms?<br>What are the impacts of plasma distribution and evolution on matrix effects and signal uncertainty?<br>What are the key factors or processes affecting signal uncertainty and matrix effects? |
| | | What are the mechanisms of laser–sample interaction leading to desirable plasma formation and evolution? | What is the impact of initial plasma formation on subsequent plasma evolution and LIBS signals?<br>What are the key mechanisms of laser–sample interaction leading to repeatable and stable plasma formation?<br>What is the impact of sample properties on plasma formation and plasma evolution? |
| | | What are the mechanisms of plasma–surrounding gas interaction leading to stable and repeatable plasma evolution? | What are the impacts of surrounding-gas properties on plasma evolution and LIBS signals?<br>What are the key factors or processes leading to unstable plasma evolution? |
| | | What is the optimal spatiotemporal signal-collection window for raw signal acquisition? | What are the best criteria for desirable signal collection, and how can the optimal spatiotemporal signal-collection window be obtained?<br>What is the impact of spatiotemporal windows on LIBS signal collection? |
| Data processing | How to transform raw signals into reliable analytical results? | What is the impact of matrix effects and signal fluctuations on analytical results? | What are the impacts of matrix effects and signal uncertainty on different types of models?<br>How do signal fluctuations propagate into analytical bias and uncertainty in different types of models?<br>How do matrix effects propagate into analytical bias and uncertainty in different types of models? |
| | | What are the principles for reducing the impacts of signal uncertainty? | What are the key preprocessing strategies for robust raw LIBS signals?<br>What are the mechanisms for reducing signal-fluctuation-induced uncertainty in quantitative analysis with different types of models? |
| | | What are the principles for matrix-effect correction and compensation? | What are the mechanisms for self-absorption correction?<br>What are the mechanisms for correcting matrix-induced bias in quantitative analysis?<br>What are the mechanisms for correcting environment-induced bias in quantitative analysis?<br>What is the role of AI technology in matrix compensation and uncertainty reduction?<br>How does AI enhance physical-principle-based models? |
| Application | How to maintain reliable analytical performance under practical constraints? | How can long-term stability and robustness be achieved? | What is the impact of slight parameter fluctuations on LIBS signals?<br>What are the key parameters for maintaining long-term stability? |
| | | How can transferability and adaptation be achieved? | How can models achieve self-adaptation and continual learning during online measurements?<br>How can models be transferred across different instrumental setups?<br>How can models be adapted when only limited real-world data are available? |
| | | How can scenario-oriented industrial deployment be achieved? | How can laboratory-level analytical conditions be approached in practical deployment? |

# 3 Fundamentals

The fundamentals of LIBS involve the coupled processes of laser–material interaction, plasma formation and evolution, ambient-gas interaction, and spectral emission. Together, these processes largely determine the precision, accuracy, and overall analytical performance of LIBS. From the perspective outlined above, this section mainly addresses the first core problem: how to obtain signals with better repeatability and reduced matrix effects. It therefore examines not only the intrinsic characteristics of the plasma itself, but also how matrix effects, self-absorption, and source-side fluctuations arise from the underlying physical processes, and how to use physical intervention to create a more stable and repeatable plasma in order to obtain more stable and repeatable signals.

## 3.1 Mechanism understanding

This section focuses on the fundamental mechanisms underlying the plasma signal source and the formation of the raw LIBS signal. It examines how matrix-related factors influence signal generation through the plasma as an intermediate state, the approaches used to address self-absorption, the spatiotemporal evolution of the plasma, and how source-side uncertainties arise during this evolution. Rather than treating these effects as isolated problems, the studies reviewed here help frame them as different parts of a coupled signal-generation process.

### 3.1.1 Matrix effect

In a broad sense, the matrix effect refers to the influence of all matrix-related factors other than the analyte content itself on the measured signal. In LIBS, these factors may be physical, such as surface roughness [10], reflectivity [11], and melting point [12], or chemical, mainly related to sample composition. In practice, these factors are coupled throughout laser ablation, plasma generation, plasma evolution, and optical emission. Matrix effects are therefore manifested in multiple forms, including nonlinear calibration behavior, signal bias, spectral interference, and pulse-to-pulse fluctuation. Correspondingly, matrix effects may be mitigated through physical approaches, or addressed through data-processing strategies. The former include surface conditioning and pelletizing, while the latter include normalization, matrix matching and data-driven modeling.

Due to the broad and inclusive nature of the matrix effect concept, the factors referred to as matrix effects can differ substantially across application domains. As a result, existing studies on matrix effects are largely domain-specific. For example, Chen et al. [13] found that moisture in coal suppresses LIBS line intensities mainly through modified ablation and plasma evolution, rather than through concentration dilution alone. Wang et al. [14] reported that preheating a Cu target enhanced LIBS emission by lowering surface reflectivity and ablation threshold, increasing the ablated mass, and raising the plasma temperature and electron density. Accordingly, many studies do not seek a universal description of matrix effects, but instead identify the dominant matrix-related factors in a specific sample system and reduce their impact through targeted compensation or experimental control. Wang et al. [10] found that, in microchip laser LIBS with an ablation crater of about 10 µm, surface roughness had little effect on spectral stability or quantitative performance once the crater overlap rate and internal-standard strategy were properly chosen. They [15] also showed that, for Al- and Fe-based metallic matrices, the severity of LIBS matrix effects depends strongly on laser defocus and spectrometer delay;

under suitable conditions, matrix interference can be mitigated by parameter optimization and pure-matrix background subtraction. These examples reflect the fact that the matrix effect is not a single physical mechanism, but rather a collective term for multiple ways in which matrix properties influence signal formation.

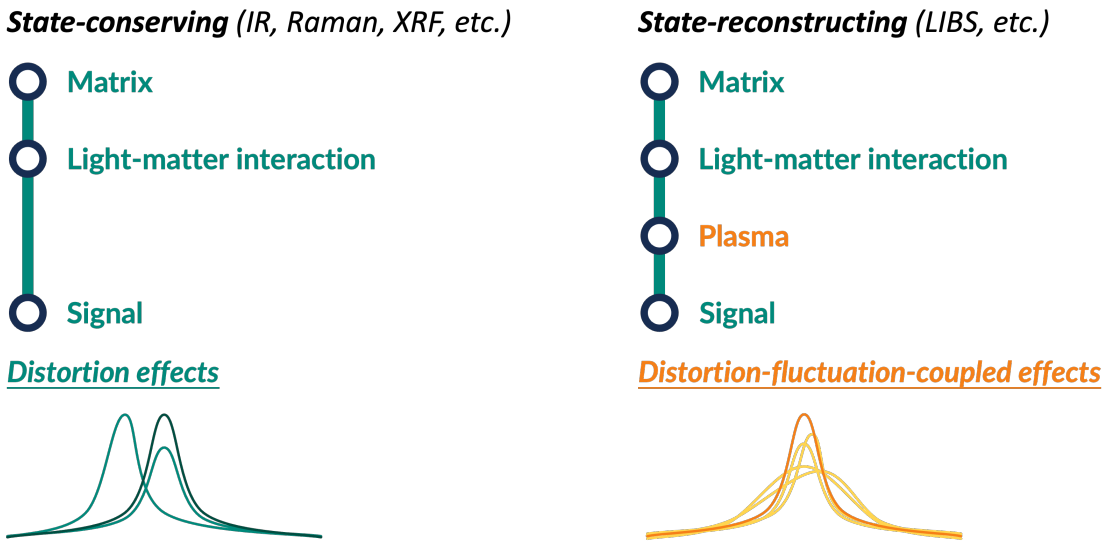


Figure 3: Schematic comparison of matrix effects from the perspective of signal generation.

To better understand the matrix effect in LIBS, this complexity can be viewed from a more general perspective of signal generation. As illustrated in Fig. 3, spectroscopic techniques may be broadly viewed as either state-conserving or state-reconstructing. In state-conserving schemes, the detected signal is generated without first reconstructing a new intermediate analytical state, and matrix effects mainly appear as distortions in the mapping from sample state to signal. LIBS, by contrast, is a typical state-reconstructing technique: the analyte is first converted into a newly formed intermediate state, namely the LIP, from which the signal is emitted. As a result, the matrix effect of LIBS is plasma-mediated and is inherently coupled with other physical processes. From this perspective, matrix effects can be re-examined along the entire analytical chain of LIBS. From sample properties through ablation, plasma evolution, and spectra to data processing and modeling, matrix effects or their resulting impacts involve two aspects: on the one hand, matrix-related variations are propagated along the chain; on the other hand, each stage may introduce new complexity due to the differences in the matrix. These two aspects are often coupled rather than isolated. At the sample level, differences in sample properties such as composition, surface roughness, reflectivity, and melting point provide the initial sources of matrix effects. At the ablation level, some of these properties, such as reflectivity and melting point, affect laser-sample coupling and thereby influence the ablated mass, crater morphology, etc. At the plasma level, these ablation-related differences further influence the initial state of the plasma and thereby influence its subsequent evolution. Additionally, because the plasma is generated from the ablated sample, matrix composition also affects plasma composition and hence its interaction with the surrounding gas. At the spectral level, these variations of plasma state are reflected in the fluctuation and distortion of spectra. Meanwhile, matrix components may also directly influence the spectra, for example by causing line overlap and molecular-band interference. At the modeling level, these effects on spectra are mapped into shifts and distortions in

the feature space, thereby affecting the quantitative performance. Therefore, these levels should be regarded as a coupled propagation chain from matrix properties to analytical results, with the plasma as the central intermediate state. This staged propagation is particularly important in LIBS because its reconstructed intermediate state is a highly transient, spatially confined, and strongly inhomogeneous laser-induced plasma. Compared with more stable plasma-based analytical systems such as ICP-MS, this small-scale and rapidly evolving intermediate state makes LIBS especially sensitive to local sample properties and short-time stochastic variations. In this sense, the spatiotemporally inhomogeneous plasma is part of the very nature of LIBS and also one of the fundamental origins of its quantitative difficulty.

Since the matrix effect is a collective term covering multiple underlying mechanisms, conventional approaches such as sample pretreatment, optimization of experimental conditions, and matrix-dependent modeling are usually specific to particular sample systems and are difficult to generalize across different matrices. In practice, one feasible route is to establish separate models for different groups of relatively similar matrices. Indeed, the validity of many LIBS studies may be inherently restricted to relatively similar matrices, such as a specific coal type or a particular alloy grade, although this limitation is often not explicitly addressed. A more general route is to modulate the reconstructed intermediate state itself, namely the plasma. Although the state-reconstructing nature of LIBS increases complexity, it also provides room for intervention: regardless of the original form or state of the sample, signal quality may in principle be improved by controlling plasma formation and evolution. From this perspective, the highly transient and spatially confined plasma of LIBS is not only a source of quantitative difficulty, but also part of its unique advantage. Compared with more stable state-reconstructing techniques such as ICP-MS, the LIBS plasma is generated locally and in situ at the sample surface, making the technique inherently more compatible with rapid, direct, and spatially resolved analysis. Although such a small-scale and rapidly evolving plasma increases sensitivity to local properties and stochastic variation, it also provides greater flexibility for engineering intervention and plasma modulation, and allows a common analytical logic to be applied to samples with very different original forms and states. This is also why plasma modulation remains a promising general direction for developing more robust and transferable LIBS methods, especially for rapid analysis in complex industrial environments.

### 3.1.2 Self-absorption effect

Self-absorption is one of the major sources of nonlinearity and spectral distortion in LIBS. It occurs when radiation emitted by atoms or ions in the plasma is reabsorbed by the same species in low-lying states. This effect reduces the observed line intensity, distorts the line profile, and may even give rise to self-reversal. Although the basic physical mechanism of self-absorption has been relatively well understood, its practical treatment remains difficult. Traditional self-absorption correction methods, such as the curve of growth (COG) and the self-absorption coefficient (SAC), can provide usable results in some cases, but their applicability and accuracy are limited by simplified assumptions and parameter requirements. Factors such as plasma inhomogeneity, complex matrices, dependence on plasma-parameter measurements, and reliance on atomic parameters may constrain the effectiveness of these traditional approaches. For these reasons, subsequent work has aimed, on the one hand, to develop more general and more accurate correction strategies, and, on the other hand, to expand toward direct methods for avoiding or suppressing self-absorption. Beyond these explicit treatments, self-absorption can also

be incorporated into broader integrated models, where it is implicitly represented as one source of nonlinearity. The following discussion is organized around four treatment strategies: correction, avoidance, suppression, and model integration.

To overcome the practical limitations of conventional self-absorption correction methods, more recent studies have aimed to reduce dependence on plasma parameter diagnostics, while retaining the physical basis of correction. Li et al. [16] proposed the blackbody radiation referenced self-absorption correction (BRR-SAC) method for calibration-free LIBS, in which self-absorption correction was achieved through an iterative algorithm constrained by the linearity of the Boltzmann plot; compared with traditional COG-based methods, this method involves no reliance on the availability or accuracy of line-broadening coefficients. Hou et al. [17] followed a similar iterative logic, using $T$ and $Nl$ as the iterative variables, and applied the method to calibration-based LIBS quantification. They [18] also proposed a self-calibrated correction method based on doublet lines within the same multiplet, which requires only the measured doublet intensities and theoretical line ratios. Xu et al. [19] extended this doublet-based self-calibration strategy to practical quantitative analysis and demonstrated improved calibration linearity and accuracy in the determination of trace elements. For non-gated detectors, Hou et al. [20] further showed that self-absorption varies during plasma evolution and therefore incorporated time-resolved self-absorption correction into a time-integration calibration-free (TICF) model, extending CF-LIBS to non-gated measurements.

A more direct way to handle self-absorption is to avoid collecting strongly affected emission in the first place, typically by selecting spatiotemporal acquisition windows in which self-absorption is intrinsically weak. Hou et al. [21, 22] proposed self-absorption-free LIBS (SAF-LIBS), in which the integration and delay time were optimized, and the measured doublet intensity ratio was compared with the theoretical value to identify time windows where the emission was close to optically thin, thereby improving quantitative accuracy. Yi et al. [23] showed by spatially resolved LIBS that self-absorption is strongly position dependent within the plasma, so that choosing appropriate collection zones can effectively mitigate its influence and improve quantification.

Self-absorption can also be suppressed by actively modifying the plasma conditions so that reabsorption becomes intrinsically weaker during plasma evolution. Wang et al. [24] showed through theoretical and experimental analysis under different background gases that self-absorption in the later stage of plasma evolution can be weakened by reducing gas pressure or using a lower-molecular-weight background gas, driving the plasma more rapidly toward optically thinner conditions. Wang et al. [25] found that a collinear double-pulse configuration could reduce self-absorption, because the gas environment created by the first pulse modifies the self-absorption behavior of the plasma generated by the second pulse. The weakest self-absorption was observed at characteristic interpulse delays for Cu, Mn, and Ni. Li et al. [26] employed laser-stimulated absorption to resonantly excite cold atoms at the plasma periphery and thereby reduce their population in the low-lying state, reducing reabsorption of center-emitted radiation and improving the linearity of calibration for minor Cu and Cr in steels.

Beyond explicit correction, avoidance, and suppression, some data-driven models in LIBS may also be regarded as an implicit way of handling self-absorption, since the effect can in principle be learned and represented by the model. Such capability, however, depends strongly on the validity of the model architecture and the representativeness of the training data. In cases of severe self-absorption, explicit correction or the incorporation of relevant physical constraints may still be necessary.

It should be noted that, in practical LIBS analysis, the treatment of self-absorption should generally be selected according to the nature of the specific problem. This selection usually involves several aspects, including the severity of self-absorption, the availability of alternative spectral lines, the possibility of optimizing the acquisition window, and the feasibility of active plasma modulation. Although it is difficult to define a universally applicable numerical threshold because self-absorption depends on multiple factors, such as the element, spectral line, plasma condition, and acquisition condition, several indicators have been used in previous studies to evaluate its severity [27, 28]. These include the self-absorption coefficient, optical depth, the deviation of measured doublet or multiplet intensity ratios from theoretical optically thin values, line-profile distortion such as abnormal broadening and self-reversal, and nonlinear saturation of calibration curves. When these indicators suggest weak or moderate self-absorption, and suitable alternative lines or spatiotemporal acquisition windows are available, avoidance strategies such as line selection and acquisition-window optimization may be sufficient [21–23]. Self-absorption may also be partly represented in data-driven models, provided that the training data are sufficiently representative of the relevant matrices, concentration ranges, and plasma conditions. In contrast, when self-absorption is strong, explicit correction, suppression, or their combination should be considered. Alternatively, less self-absorbed lines may be used if available, although additional measures are often required to ensure adequate sensitivity, SNR, and freedom from spectral interference.

### 3.1.3 Plasma characteristics investigation

The study of plasma spatiotemporal evolution has directly deepened our understanding of the plasma that serves as the signal source in LIBS. Such studies generally follow two main approaches. One relies on numerical simulations to provide intuitive insight and physically interpretable conclusions, while the other employs time- and space-resolved diagnostics to obtain a more realistic and physically grounded picture of plasma evolution.

Oderji et al. [29] developed a simulation program to investigate the non-equilibrium phase-explosion mechanism in nanosecond laser ablation, and compared the model predictions with experimental results for tungsten under vacuum conditions. Their model suggested that the vapor and particles generated during ablation shield the target from subsequent laser energy deposition. This mechanism was validated by mass measurements using a quartz crystal monitor and by time-resolved optical emission spectroscopy, with the simulation results showing good agreement with the experiments.

Fu et al. [30] investigated time-resolved Bremsstrahlung and spectral emission in the early-stage tungsten plasma generated by nanosecond laser ablation. Combining a one-dimensional model with experiments, they showed that Bremsstrahlung dominates in the initial stage and decays exponentially, whereas W I emission lines gradually intensify and W II lines first increase and then decrease. This study highlighted the importance of continuum radiation in LIBS for diagnostics of fusion plasma-wall interactions.

He et al. [31] proposed a three-step method for reconstructing transient images of LIP plumes. This method successfully reproduced experimental images, yielded reliable distributions of plasma parameters, and identified the radiation sources of ions in different wavelength bands. Their work provided a useful means for plasma diagnostics by integrating image reconstruction with spectral simulation.

Cai et al. [32] carried out LIBS analysis of coal samples with different volatile contents in an argon atmosphere. Using a high-speed camera, they captured the temporal and spatial evolution of plasma emission during plasma development. They analyzed the

spatiotemporal distributions of atomic emissions (C, H, O, N), ionic emissions (Ca II), and molecular emissions ($CN, C_2$) spectra of the plasma, together with plasma temperature and electron density. Their results revealed the mechanism by which the preferential vaporization of volatile components influences plasma generation and evolution. On this basis, they proposed a conceptual model of laser-matter interaction, providing a theoretical basis for interference correction in LIBS analysis of coal.

### 3.1.4 Uncertainty generation

Just as repeatedly emphasized in earlier reviews [1, 5–7, 9, 33, 34], one of the major bottlenecks in LIBS quantification is the limited measurement accuracy caused by signal uncertainty. Based on plasma diagnostics and an improved physical understanding of LIBS plasma, researchers have made important progress in clarifying the mechanisms responsible for signal uncertainty. These advances have also provided physically grounded directions for uncertainty reduction in LIBS.

Fu et al. [35] were the first to systematically quantify the contributions of fluctuations in core plasma parameters to LIBS signal uncertainty by combining spectroscopic and imaging diagnostics. They simultaneously recorded the spatiotemporal evolution of spectra and images from a titanium-alloy plasma. Through error-propagation analysis, they resolved the individual contributions of parameter fluctuations at different stages of plasma evolution to the signal RSD. The observed spectral uncertainty was decomposed into the combined effects of fluctuations in temperature $T$, electron density $n_e$, and total number density $n_s$. Their results showed that fluctuations in $n_s$ contributed most strongly to the RSD within the commonly used acquisition window. Combined with the imaging results, they further showed that plasma morphological fluctuations are likely the main source of the fluctuations in $n_s$, and thus the dominant physical origin of signal RSD.

Building on this quantitative picture, Fu et al. [36] further designed a multi-camera continuous-imaging experiment to reveal the dynamic physical origin of uncertainty generation. Using three complementary metal-oxide-semiconductor (CMOS) cameras, they synchronously captured three consecutive images of the same plasma during the early stage of evolution at the sub-microsecond scale, thereby directly tracking the emergence of morphological fluctuations. From these image data, they calculated a morphological correlation coefficient and found that initially small morphological perturbations were amplified at a critical delay of 150–200 ns. Combined with theoretical analysis, they attributed this amplification to the shock-wave-driven rebound of the plasma front and its subsequent collision with the underlying plasma, thus providing a mechanistic explanation for the strong fluctuations in $n_s$ identified in the previous study.

After the dominant factors and their generation mechanisms had been clarified, Gu et al. [37] further refined the error-propagation-based analysis of LIBS signal uncertainty by improving plasma diagnostics with a self-absorption-aware spectral-fitting model and by explicitly accounting for parameter intercorrelations. They modified the spectrum-fitting model used in the previous study to consider self-absorption, and applied it to time-resolved spectra of copper plasma to retrieve plasma parameters more reliably. On this basis, they performed full error-propagation analysis, reconfirming the central role of fluctuations in columnar total number density $Nl$ throughout plasma evolution, quantifying the substantial negative contribution arising from the $T - Nl$ correlation term, and showing that self-absorption suppresses the magnitudes of the major uncertainty-contribution terms. This analysis also provided physically meaningful guidance for reducing signal uncertainty.

Table 2: Comparison between signal enhancement and plasma modulation in LIBS.

| | Plasma modulation | Signal enhancement |
|---|---|---|
| Objective | Multi-objective: signal repeatability as the main purpose, simultaneous signal intensity enhancement, and matrix-effect reduction in some cases, for better quantitative performance and higher detection sensitivity. | Single-objective: enhancement for higher detection sensitivity. |
| Underlying logic | 1) Process-oriented: achieves the coordinated optimization of multiple indicators through active and targeted regulation of the process of plasma formation and evolution.<br>2) Produces a more stable/repeatable plasma, often accompanied by a longer plasma lifetime or stronger emission, by modulating plasma evolution. | 1) Result-oriented: mainly focuses on the final signal output performance and lacks systematic regulation of the plasma evolution process.<br>2) Extends the lifetime of the plasma and increases the ablated mass for a stronger plasma, usually by introducing additional energy. |
| Approaches | Currently effective methods include confinement, beam shaping, flame-assisted modulation, and gas-mixture plasma modulation; other enhancement methods need further investigation. | Nanoparticle-enhanced LIBS, double-pulse LIBS, magnetic-field-assisted enhancement, surface-assisted enhancement, and other intensity-enhancement strategies. |

## 3.2 Plasma modulation: an upgraded concept beyond signal enhancement

This section focuses on how to actively control the plasma signal source. Plasma modulation here refers to the active manipulation of plasma evolution by altering external factors, rather than mere signal enhancement in the narrower sense. A comparison between these two paradigms is provided in Table 2. These strategies aim to directly intervene in the physical process in order to improve signal stability, enhance signal intensity, and mitigate the non-ideal effects at the source side. Detailed discussions of these modulation methods are available in a recent review [38].

### 3.2.1 Spatial confinement

Before Wang et al. reclassified spatial confinement, together with other enhancement strategies, as a plasma modulation approach in their 2021 review [9], it was often regarded simply as an isolated signal-enhancement technique. It involves placing cavities of different geometries around the plasma to modulate plasma evolution and the associated emission characteristics. Most earlier studies on spatial confinement mainly aimed at signal enhancement and the optimization of experimental conditions from that perspec-

tive. Wang et al. [39] were the first to show that cylindrical confinement could reduce signal RSD, indicating improved shot-to-shot reproducibility of plasma morphology. Fu et al. [40] further observed, through synchronized imaging of plasma plumes and shock waves, that reflected shock waves compressed the plasma at the confinement boundary, suggesting that the signal enhancement originated from a denser plasma core and a higher plasma temperature induced by shock-wave compression. This mechanism also implies that the reflected shock wave can help stabilize the plasma position and shape, providing a theoretical basis for the reduction in RSD under spatial confinement. From the perspective of the current understanding of LIBS plasma, this can be regarded as an early sign of the transition from signal optimization toward control of the underlying physical process. Since unconfined shock waves, as discussed in Section 3.1.4, contribute to fluctuations in plasma shape, it is then a natural step to use spatial confinement to redirect this effect toward more uniform plasma compression.

In recent years, advances in spatial confinement have mainly involved cavity optimization, application to specific scenarios, and combination with other plasma modulation methods. For example, Jia et al. [41] showed that, for cylindrical cavities, the strongest enhancement was obtained when the laser was focused at the cavity center, which is consistent with the proposed mechanism of uniform circumferential compression by reflected shock waves. Chen et al. [42] applied cylindrical spatial confinement to particle-flow detection and showed that the confinement device could effectively compress the plasma, suppress air excitation, and improve signal stability. Qiu et al. [43] combined spatial confinement with dual-pulse excitation, achieving up to a 4.1-fold increase in the emission intensity of Fe, Ni, and Cr, together with reduced spectral fluctuations.

### 3.2.2 Beam shaping

Beam shaping refers to manipulating the spatial energy distribution of the laser beam using optical elements. In this way, the incident beam can be transformed from its original Gaussian profile into a flat-top, circular, or other customized energy distribution. Although the direct object of control in beam shaping is the incident laser rather than an already formed plasma, it affects the ablation behavior and thus modifies the initial conditions of plasma generation. Moreover, in conventional ns-LIBS, plasma formation often occurs within the duration of the laser pulse, so the later part of the pulse may continue to interact with the initial plasma. Therefore, from this perspective, beam shaping participates in the early stage of the LIP life cycle and serves as an upstream plasma modulation strategy acting at the plasma-generation stage.

Hou et al. [44] explained and demonstrated signal improvement using a flat-top beam. In a Gaussian beam, the energy density is highest in the central region, which can produce excessively high temperature and electron density in the plasma core. This in turn promotes plasma shielding and hinders further laser energy deposition into the core. In addition, the resulting spatial inhomogeneity of plasma parameters can increase initial fluctuations in plasma morphology. By contrast, the flatter energy distribution of a flat-top beam weakens plasma shielding and enables more effective laser–plasma energy coupling, thereby enhancing the signal. At the same time, it makes the plasma parameter distribution more uniform, leading to improved signal reproducibility. They reported a signal enhancement by a factor of 1.5–3.5, together with an approximately 50% reduction in RSD at medium to high laser energies ($\geq$ 30 mJ). Through combined theoretical and experimental analyses, they demonstrated that beam shaping can serve as an active means of plasma modulation.

Li et al. [45] generated various beam profiles using a spatial light modulator, including Gaussian, flat-top, circular, inverse-conical, and arrow-target patterns. Significant enhancement of both atomic and ionic emission lines was observed for pure aluminum and pure copper, with enhancement factors of 3–6 and an approximately 50% reduction in RSD. Based on time-resolved spectroscopy, they suggested that beam shaping helps optimize energy deposition, while plasma imaging revealed a more compact plasma core. They further applied beam shaping to a complex sample, namely bearing steel. Under the inverse-conical mode, the detection limits of elements such as Cr and Mn were reduced by about sixfold, and the signal-to-noise ratio increased by up to 7.7 times, further demonstrating the effectiveness of this strategy for complex samples.

### 3.2.3 Surrounding gas control

Throughout its lifetime, LIBS plasma undergoes intense interactions with the surrounding gas. Numerous studies have investigated how LIBS spectral signals are affected by the type and pressure of the surrounding gas [46, 47]. However, many of these studies have remained largely descriptive and have not provided a unified mechanistic understanding. As a result, inconsistent conclusions have sometimes been reported under different experimental conditions, limiting their practical value as guidance. Recently, building on a refined mechanistic understanding of plasma-gas interactions, researchers have begun to elucidate, within a unified framework, how various surrounding gas parameters, including pressure, temperature, and gas-specific properties (e.g., molecular weight and ionization energy), influence LIBS plasma evolution. This has provided a more general guiding principle for plasma modulation through surrounding gas control.

Zhang et al. [48] showed that the inconsistencies reported in previous studies on the effect of background-gas pressure on LIBS signals may arise from non-standardized spatiotemporal acquisition windows. When different acquisition windows are used, the dependence of LIBS signals on pressure may appear different. By optimizing the spatiotemporal window at each pressure, they found that reducing the pressure, on the one hand, weakens the collision, mixing, and shock-wave generation processes between the plasma and the surrounding gas, thereby improving the morphological stability of the plasma. On the other hand, it also weakens the confinement imposed by the surrounding gas, leading to excessive plasma expansion and a lower particle density in the signal-collection region, which in turn results in a relatively low SNR. Under the combined action of these two effects, the RSD of the LIBS signal exhibits a U-shaped dependence on pressure, first decreasing and then increasing.

Studies directly addressing the influence of surrounding gas temperature on LIBS signals remain relatively scarce. Most previous work has focused on signal enhancement by flames or micro-torches [49–51]. Song et al. [52] further examined how temperature affects the physical evolution of LIBS plasma. Based on plasma imaging, they found that the rebound process within the plasma is weakened in a high-temperature flame, possibly because the higher local sound speed reduces the Mach number and thus weakens the shock-wave intensity. As a result, the plasma morphology becomes more stable. In experiments on brass samples, the RSD of Cu atomic emission lines was reduced from about 10% to around 6%. They also investigated the mechanism of flame-induced signal enhancement and found that the dominant factor was sample heating, with reduced plasma energy dissipation playing a secondary role.

The molecular weight, ionization energy, specific heat ratio, thermal conductivity, and other properties of the surrounding gas are intrinsically coupled through gas identity.

Song et al. [53, 54] employed a neural-network approach to decouple the effects of key ambient-gas properties on LIBS signals. They designed 720 gas mixtures based on six pure gases (He, Ne, Ar, $O_2$, $N_2$, $CO_2$) and carried out experiments in these atmospheres to train a Kolmogorov-Arnold network (KAN) model that maps ambient-gas properties to LIBS signal intensity and RSD. The trained model was then used to generate model-predicted data with independently varied gas properties, and these virtual datasets were used to reveal the separate effects of individual properties. The results showed that a higher $\gamma$ improves both signal intensity and repeatability; a higher $M$ enhances signal intensity but deteriorates repeatability; and an appropriate increase in $E$ can significantly improve both repeatability and intensity, whereas excessively low or high $E$ may deteriorate repeatability, and excessively high $E$ may also reduce signal intensity. Analysis of time-resolved spectra and plasma images further revealed distinct underlying mechanisms. In high-$\gamma$/low-$M$ environments, the improved repeatability arises from weaker shock waves associated with higher sound velocity, whereas in high-$E$ environments, it arises from a weakened counter-pressure process associated with a higher plasma core position. For signal intensity, the dominant pathways are property-dependent: higher $\gamma$ reduces thermal loss, higher $M$ promotes laser-energy absorption, and appropriate $E$ suppresses excessive ionization of the ambient gas and improves energy allocation to the sample species.

#### 3.2.4 Other modulation methods

Besides the modulation methods discussed above, a number of additional plasma modulation methods have been reported, including magnetic confinement, double-pulse [55], microwave assistance, spark discharge, and surface enhancement. These approaches intervene in plasma evolution through different physical pathways. For clarity, Table 3 provides a comparative summary of plasma modulation methods, focusing on their physical mechanisms, reported plasma responses, and analytical signal impacts.

Table 3: Comparison of plasma modulation methods in LIBS.

| Modulation Methods | Physical Mechanism | Sample | Reported Changes on Plasma Parameters | Reported Signal Impact | Notes | Remarks | Ref. |
|---|---|---|---|---|---|---|---|
| Spatial confinement | Confining plasma expansion via shock wave reflection at physical boundaries | Bituminous coal powder pellet | $T$ ↑34%–37% & $n_e$ ↑2.2–2.7× | C I 193.09 nm: EF 2 & RSD ↓21%–36% | | Geometry-dependent | [39] |
| | | Bituminous coal powder pellet | $T$ ↑∼20% & $n_e$ ↑∼2× | C I 193.09 nm: RSD ↓21%–30% | | | [56] |
| | | Steel | Not reported | V I 440.85 nm: EF 4.2 | | | [57] |
| | | Silicon wafer | $T$ ↑∼16% & $n_e$ ↑∼16% | Si: EF 1.5–2.9 & RSD ↓36%–75% | Spatial confinement + collinear dual pulse | | [58] |
| | | Air | Not reported | N, O: EF 1.5–2.9 & RSD ↓∼25% | | | [59] |
| | | Brass | Plasma compressed | Not reported | | | [40] |
| Beam shaping | Affecting laser-sample interaction and initial plasma evolution | Steel | Not reported | Mn, Cr: EF <1 & RSD ↓18%–46% | | Shaping optics required | [60] |
| | | Magnesium alloy | $T$ ↑39% & $n_e$ ↑ | Mg, Si, Al: EF 1.5–3.5 & RSD ↓∼50% | | | [44] |
| | | Uranium ore | $T$ ↑10%–40% & $n_e$ ↑2%–3% | U II 409.013 nm: EF 5 & RSD ↓∼50% | | | [61] |
| Surrounding gas control | Controlling plasma–surrounding-gas collision processes | Steel | $T$ ↑∼4% & $n_e$ ↓17%–↑50% | Mn I 404.136 nm: EF 5 | Micro torch | Gas supply required | [49] |
| | | Titanium alloy | $T$ ↓1%–↑10% & $n_e$ ↓2%–↑3% & $n_s$ ↑2–10× | Ti I 498.173 nm: EF 9 & RSD ↓45% | He, Ne, Ar mixture | | [62] |
| | | Brass | $T$ ↑∼6% & $n_e$ ↓∼22% | Fe, Pb, Cu, Zn: EF ∼2 & RSD ↓40% | Flame | | [52] |
| Magnetic confinement | Confinement by Lorentz force | Metal & alloy | Plasma compressed | Co I 345.35 nm: EF ∼22<br>Cr I 425.44 nm: EF ∼24 | Spatial confinement + magnetic confinement | Systematic understanding lacking | [63] |
| | | Aluminium alloy | $T$ ↑∼44% & $n_e$ ↑∼15% | Al, Li: 1.5∼3 | | | [64] |
| | | Copper | $T$ ↓ | Cu: 3∼8 | | | [65] |
| | | Polycrystal tungsten | $T$ ↑ & $n_e$ ↓∼40%–↑∼30% | W: EF ∼1.4 | | | [66] |
| Dual pulse | Plasma reheating or re-excitation | Steel | Not reported | Fe: EF 5.5–16 & RSD ↓∼60% for reheating<br>Fe: EF 3.2–7.9 & RSD ↓5%–↑68% for pre-ablation | | Timing-sensitive | [67] |
| | | Aluminium alloy | lifetime ↑ | Al I 308.2 nm: EF 9 & RSD ↓56% | | | [68] |
| | | Air | $T$ ↑4–16% | Not reported | | | [69] |

Continued on next page

Table 3: Comparison of plasma modulation methods in LIBS (continued).

| Modulation Methods | Physical Mechanism | Sample | Reported Changes on Plasma Parameters | Reported Signal Impact | Notes | Remarks | Ref. |
|---|---|---|---|---|---|---|---|
| | | Aluminium alloy | Not reported | Ni, Cr, Fe, etc.: EF 3∼28 & RSD ↓22%–76% | | | [70] |
| | | Aluminium alloy | $T$ ↑ & $n_e$ ↑ | Al II 281.62 nm: EF ∼7<br>Li I 610.37 nm, Mg I 518.36 nm: EF ∼4 | Circular and annular dual pulse | | [71] |
| Microwave assisted | Sustained plasma excitation via electromagnetic-wave energy coupling | Potassium feldspar powder pellet | Not reported | Na, K: FWHM ↓43%–53% | Self-absorption reduced | Microwave generator required | [72] |
| | | Brass | $T$ ↑8% & $n_e$ ↑21% vs. LIBS<br>$T$ ↑4% & $n_e$ ↑7% vs. MA-LIBS | Cu, Zn, Fe, Pb: EF 1.08–1.28 vs. LIBS<br>& RSD ↓30%–41% vs. MA-LIBS | With spatial confinement | | [73] |
| | | Aluminium, iron, ceramics | $T$ ↑ & $n_e$ ↑ | Al I 396.15 nm: EF ∼2.67 & RSD ↓∼54% vs. 1000 W | 1000 W–3000 W | | [74] |
| Spark discharge | Energy injection via high-voltage electric field | Silicon wafer | Not reported | Si II: EF 52 & RSD ↓50%–60% | | High-voltage power supply required | [75] |
| | | Bituminous coal powder pellet | $T$ ↓ & $n_e$ ↓ for spark discharge<br>$T$ ↑ & $n_e$ ↑ for spark discharge + spatial confinement | C I 193.09 nm: EF 2.4 & RSD ↓∼39% | Spark discharge + spatial confinement | | [76] |
| | | Silicon wafer & soil | $T$ ↑∼17% & $n_e$ ↑∼2× | Si I 390.55 nm: EF 13.8<br>Cd II 214.44 nm: EF 2.3 | | | [77] |
| | | Brass | $T$ ↑ & $n_e$ ↑ | Cu I 515.3 nm: EF >10 | Spark discharge + nanoparticle enhancement | | [78] |
| Surface enhancement | Absorption enhancement or local field amplification | Titanium alloy, brass, silicon wafer | Not reported | Ti: EF 1–15, RSD ↑20%–100%<br>Cu: EF 1.2–4.7, RSD ↑1–2×<br>Si: EF 2–5.4, RSD ↓33%–↑100% | Pre-ablation / no pre-ablation | Surface treatment required | [79] |
| | | Brass | $T$ ↑ & $n_e$ ↑ | Cu I 515.3 nm: EF >10 | Spark discharge + nanoparticle enhancement | | [78] |
| | | Oil | Not reported | Mg, Ca: EF 12–22 & RSD ↓∼70% | Quantum dots | | [80] |

# 4 Instrumentation

The fundamental understanding of LIBS helps to clarify the formation mechanism of the signal source and why the original signal often deviates from the ideal state. Further progress also depends on instrumentation capable of operating under practical conditions. This section mainly discusses the third core problem, namely how to maintain reliable analytical performance under practical deployment constraints, while also being related to the first core problem through signal generation and collection. In this sense, the requirements and limitations of practical deployment shape the LIBS analytical process through individual components, platform integration, and scenario-oriented instruments. From this perspective, this section reviews the latest progress made in China in LIBS system components, integrated LIBS systems, and tandem technologies.

## 4.1 LIBS system components

The performance and versatility of a LIBS instrument depend strongly on the design and configuration of its individual components. From the laser source and optical arrangement to the spectrometer and detector, each subsystem affects a different stage of signal acquisition, including plasma generation, emission collection, and spectral detection. During these stages, several engineering parameters play a particularly crucial role and are closely related to the quantitative performance of LIBS. For the laser source, the stability of pulse energy and the repeatability of focusing distance directly affect the coupling of the laser with the sample and the stability of plasma formation. For the optical arrangement, the alignment stability and the collection geometry will influence the repeatability of emission collection. For the spectrometer and the detector, the spectral resolution and the detector sensitivity determine the basic capabilities for line separation and weak signal detection, while the wavelength stability, detector response stability, noise level and timing accuracy affect the long-term consistency of spectral acquisition. These parameters largely determine the quality and repeatability of the raw signals, and subsequent calibration and modeling rely on these signals. Continuous optimization at the component level has therefore remained a fundamental route for improving the analytical capability of LIBS systems.

In the early development of LIBS in China, many key components were largely supplied by foreign manufacturers, and component-level innovation was also led mainly by overseas groups. Over the past decade, however, substantial progress has been made in domestic LIBS instrumentation. Chinese manufacturers have gradually developed core components such as spectrometers, detectors, and laser sources, while Chinese researchers have also carried out studies on optical-path design and application-oriented components to improve quantitative performance and enhance practical applicability. Nevertheless, despite this rapid progress, the overall engineering maturity of domestic LIBS instruments, especially in terms of long-term stability, robustness, and consistency, still has not fully reached the level of the most established overseas systems.

One representative direction is the development of compact laser sources. Zhang et al. [81] developed a portable, high-peak-power passively Q-switched Nd:YAG laser with a maximum pulse energy of 10 mJ and a pulse width of about 2 ns, corresponding to a peak power of 5 MW. The laser head was 65 mm long and 25 mm in diameter. A pulse-energy RSD below 0.2% was obtained without any cooling system. Such compact laser sources are favorable for portable LIBS instrumentation, and have also been explored in

application studies such as blood-serum analysis [82].

Chinese researchers have also explored compact optical designs for enhancing plasma excitation and signal acquisition. Xu et al. and Yang et al. [83, 84] proposed a single-beam-splitting (SBS) configuration, in which one laser pulse is divided into two sub-pulses by a beam splitter. By optimizing the incident geometry, this design enhanced the intensities of Al and Cu emission lines by factors of 5.6 and 4.8, respectively, while also extending the plasma lifetime. The SBS configuration was further combined with calibration-free LIBS and self-absorption correction to enable quantitative analysis of copper alloys, with relative errors ranging from -17% to +12%.

## 4.2 Integrated LIBS systems

In addition to the optimization of individual components, the overall performance and applicability of LIBS also depend on how these components are integrated into a coordinated and stable system.

The development of integrated LIBS platforms has been one of the most significant advances in LIBS instrumentation in China over the past decade, with major efforts devoted to compactness, automation, and adaptability to diverse analytical environments. Such system-level integration is an essential step toward practical deployment. For convenience, the representative systems reviewed here are grouped into portable, standoff, and online configurations according to their dominant deployment characteristics. This classification is not intended to be strictly exclusive, since a single platform may combine multiple attributes.

Portable LIBS systems have been primarily driven by the growing demand for rapid, on-site, and in-situ analysis in field and industrial environments. In contrast to laboratory-based analytical methods, which often involve sample collection, transport, and pretreatment and place greater emphasis on quantitative accuracy, portable LIBS aims to minimize sample preparation and shorten analytical turnaround time. Zha et al. [85] reported a portable bench-top LIBS analyzer capable of delivering 100 mJ laser pulses with a pulse width of 10 ns in a compact format. Zhang et al. [86] integrated spectral preprocessing, dimensionality reduction, and machine-learning models into a portable LIBS device, enabling rapid classification of seven raw rock samples (e.g., shale and basalt) at a petroleum logging site with an accuracy of 98%. Gu et al. [87] incorporated spatial confinement into a mobile LIBS platform for on-site detection of heavy metals in soil, achieving a detection limit of approximately 8 ppm. Cai et al. [88] also demonstrated the use of portable LIBS for in-situ identification of power-plant boiler-tube materials and assessment of their aging state.

Standoff LIBS systems have been developed to enable safe, non-contact elemental analysis in high-temperature, hazardous, or otherwise inaccessible environments. Pan et al. [89] developed a series of commercial LIBS analyzers that were integrated into the process flow of high-temperature melts (>1000 °C), enabling remote online monitoring of molten-metal composition and subsequent process control. Sun et al. [90, 91] combined a Cassegrain telescope with dual-pulse laser configuration to construct a LIBS system for in-situ monitoring of molten steel and molten magnesium alloys, achieving RSDs reduced to 2%–3% and below 10%, respectively. Cheng et al. [92] achieved remote identification of bacterial samples at a distance of 3 m by incorporating a Cassegrain reflecting telescope in the LIBS optical system. The classification accuracy exceeded 99%, highlighting the potential of standoff LIBS for non-contact biological analysis.

Online LIBS systems have been motivated by the need for continuous, real-time quality monitoring and process control in industrial production. These systems emphasize deep integration with the production process, reducing the time delays and representativeness issues associated with offline inspection through automated operation and real-time analysis. Yao et al. [93, 94] developed an online LIBS system for coal powder flow that integrates direct particle-flow analysis, high-speed continuous spectral acquisition, real-time spectral screening and correction, and artificial-neural-network- or partial-least-squares-based modeling for online prediction of coal-quality parameters. Liu et al. [95] integrated LIBS with a programmable logic controller (PLC), achieving RSD of 0.98%, 2.36% and 21.02% in the monitoring of aluminum, magnesium and iron in molten zinc, respectively.

## 4.3 Tandem technology

With the advancement of LIBS, it is increasingly being combined with complementary analytical techniques to enhance its capability for trace element detection, provide supplementary information on the molecular structure, enable rapid elemental mapping, or directly improve quantitative precision and accuracy. According to the degree of integration at the instrumental level, Yao et al. [96] classified the measurement schemes of LIBS-based spectral tandem technology into two categories: synchronous measurement and sequential measurement. In sequential measurement, the two modalities acquire signals independently, and their coupling is mainly reflected at the level of data fusion. Such schemes do not necessarily require an integrated instrument, as the two measurements can be performed separately using independent systems. When an integrated setup is adopted, it usually consists of two relatively independent measurement modules together with a sample translation stage. Representative examples include combinations with XRF, near-infrared spectroscopy (NIRS), and hyperspectral imaging (HSI). In synchronous measurement, by contrast, the two modalities are more tightly integrated at the instrumental level and often share part of the excitation or collection subsystems. Representative examples mainly include combinations with laser ablation inductively coupled plasma mass spectrometry (LA-ICP-MS), laser-induced fluorescence (LIF), and Raman spectroscopy. More detailed introductions to these tandem techniques are also available in the review [96]. It should be noted that the integration of different techniques does not by itself guarantee the reliability of multimodal fusion. To enable the model to exploit physically meaningful complementary information rather than merely statistical correlations, the sampling regions, detection depths, spatial positions, and, when relevant, acquisition times of different modalities should be carefully considered. For LIBS combined with molecular spectroscopies such as Raman spectroscopy or NIRS, same-point or spatially matched measurements are desirable. Since molecular spectroscopies are usually non-destructive whereas LIBS is locally micro-destructive, molecular spectra are generally acquired before LIBS in same-point surface analysis; in stratigraphic analysis, LIBS may instead be used first to expose deeper layers for subsequent molecular spectroscopic detection.

For LIBS-LIF and LIBS-LA-ICP-MS, the two modalities are directly linked through the same laser-induced ablation event, which provides an intrinsic physical correlation between the two datasets. Such synchronous schemes, however, also require precise temporal coordination to ensure excitation or signal acquisition within the appropriate time window. Dong et al. [97, 98] developed a lab-built LIBS-LA-ICP-MS hybrid system for elemental analysis of coal, enabling simultaneous determination of major and minor

elements by LIBS and trace elements by LA-ICP-MS. Li et al. [99–102] constructed a lab-built LIBS-LIF hybrid system for trace-element analysis in alloys and soils.

LIBS-Raman systems are usually characterized by a relatively high degree of instrumental integration, as the two techniques can share the laser source, part of the optical path, and even the spectrometer. Raman spectroscopy provides molecular information that complements the elemental information obtained by LIBS. Guo et al. [103] constructed a lab-built LIBS-Raman hybrid system, in which the LIBS signal of $Na^+$ and the Raman signal of $SO_4^{2-}$ were simultaneously detected. Sun et al. [104] developed a same-point alternating LIBS-Raman method for the stratigraphic analysis of murals, in which LIBS was used to ablate successive pigment layers and Raman spectroscopy was subsequently performed at the bottom of the same ablation crater. This design established a depth-resolved correspondence between LIBS elemental signals and Raman molecular fingerprints, allowing realgar and orpiment layers to be distinguished and their thicknesses to be estimated.

# 5 Data processing and modeling

Due to the complexity of the relationship between LIBS signals and analytical targets, the transformation from raw signals into reliable analytical results depends on effective data preprocessing and robust modeling. This section mainly addresses the second core problem, namely how to achieve this transformation, typically by reducing the effects of matrix and signal uncertainty. From this perspective, the following sections review recent progress in China on LIBS data preprocessing, classification and quantification, as well as multimodal modeling strategies associated with tandem techniques.

## 5.1 Data preprocessing

Data preprocessing is the crucial first step in the LIBS data analysis process, directly influencing the performance of subsequent classification and quantitative models. Due to the highly non-uniform spatiotemporal characteristics of the plasma and the inherent heterogeneity of the samples, LIBS spectra are often subject to baseline fluctuations and environmental noise arising from various physical mechanisms. Appropriate screening and correction of these interfering signals are essential for the subsequent establishment of models to capture the authentic correlation. This section reviews recent progress in data preprocessing in China, highlighting a trend that combines physical insights with statistical criteria or machine learning algorithms.

### 5.1.1 Noise suppression and drift correction

Over the past decade, there have been only limited fundamental methodological advances in filtering, denoising, and baseline correction [105–107]. These techniques and their refinements have become relatively mature in both theoretical understanding and engineering practice. Further improvements in such methods are therefore unlikely to substantially enhance continuum-background correction in LIBS. For noise suppression and drift correction, researchers have gradually shifted their attention from random spectral noise and continuous background interference toward systematic drift over longer time scales.

Hao et al. [108, 109] applied conventional filtering and denoising methods to improve long-term repeatability and adapted these methods for that purpose. They introduced a Kalman-filter-based approach for calibration updating and proposed a two-dimensional wavelet denoising method, which reduced the spectral RSD by up to 37%.

Zhou et al. [110] proposed a long-term drift-correction method that combines an internal standard with dominant factor partial least squares (PLS). They quantified spectral fluctuation using an intensity-ratio drift metric and then established a correction model relating spectral intensity to this drift metric using PLS. Using nine days of measurements for major elements in alloy steel, including carbon, silicon, chromium, nickel, copper, and manganese, the root mean squared error (RMSE) of each element decreased by approximately 50%, while the RSD decreased by 20% to 50%.

Liu et al. [111] proposed a correction method based on laser beam intensity. They first preprocessed both the beam-intensity distribution curve and the spectral intensity, and then used a partial least squares regression (PLSR) model to establish the relationship between the relative deviation in beam intensity and that in spectral intensity. In measurements collected over more than 30 days for copper and silicon samples, the long-term RSD decreased from approximately 13.5% to 4% and from approximately 10.7% to 6.5%, respectively.

### 5.1.2 Normalization and signal stabilization

Normalization and signal stabilization aim to compensate for plasma fluctuations and experimental variability. Conventional methods mainly include spectral area normalization [112] and internal calibration [113]. In recent years, related studies in China have increasingly explored physics-informed correction and multimodal signal integration.

One line of research uses plasma acoustic signals as auxiliary information for normalization. Zheng et al. [114] coupled LIBS with quartz tuning forks for plasma acoustic signal acquisition, leveraged the narrowband resonance characteristics and high signal-to-noise ratio of the quartz tuning fork to correct spectral intensity, and applied the corrected signals to the construction of multivariate calibration models. Tang et al. [115] acquired spectral and acoustic signals simultaneously, analyzed the relationship between acoustic energy and material grain size, and proposed an acoustic–spectral information fusion strategy, achieving discrimination among grain-size classes through feature selection and classification models. Zhou et al. [116] introduced temperature and pressure parameters obtained from acoustic shock-wave inversion into the spectral normalization process, proposed a physical-information genetic algorithm (PIGAs) framework, and corrected spectral intensity under varying laser energy conditions.

The spectrum standardization method proposed by Wang et al. [117] normalizes spectral lines on the basis of physical principles. Its basic idea is to convert the measured line intensity into the hypothetical emission intensity at a reference temperature, electron density, and total number density. In the original spectrum standardization method, plasma parameters are first derived from the spectrum, using atomic parameters together with the Boltzmann plot and Stark broadening, and are then used to explicitly normalize spectral lines to a standard temperature and degree of ionization. The total number density is determined from the intensities of the target-element spectral lines together with an additional compensation term. The simplified spectrum standardization method [118] directly corrects the deviations in spectral intensity caused by plasma-parameter fluctuations, without explicitly solving for the plasma parameters. In recent years, within the framework of spectrum standardization, Gu et al. [119, 120] developed the total

number density compensation (TNDC) method, which employs a weighted sum of spectral lines to more precisely compensate for fluctuations in total number density. To address severe matrix-induced spectral interference, Ji et al. [121] adopted the assumption of stoichiometric ablation and instead used the spectral lines of matrix elements for total number density correction.

Plasma images have also been used as supplementary information for normalization. Zhang et al. proposed a series of LIBS spectral-intensity correction methods based on feedback from plasma image information. In these studies, spectral intensity was corrected using plasma position information [122], principal components extracted from plasma images [123], and plasma information obtained from orthogonal-direction imaging [124]. The effectiveness of these methods was verified in the quantitative analysis of alloy and slurry samples. Guo et al. [125, 126] further integrated plasma image information into the framework of spectral normalization. They used the area of the plasma region in the image to represent the total number density, the image brightness to represent the temperature, and a histogram-of-oriented-gradients descriptor to characterize the influence of plasma morphology.

### 5.1.3 Data screening and feature selection

LIBS data analysis still faces challenges from invalid or poor-quality spectra and redundancy in high-dimensional features, both of which can compromise model robustness and interpretability. Data screening and feature selection therefore seek to obtain more consistent and informative representations of LIBS data through statistical criteria, physical constraints, or data-driven methods, thereby providing more reliable inputs for subsequent classification and quantitative modeling. In recent years, these strategies have shown a growing tendency to combine physical insight with statistical and machine-learning-based methods.

Chen et al. [127] developed a plasma-image-based data screening method to identify valid spectra and improve spectral stability in LIBS. Compared with using the intensities of selected spectral lines as reference indicators, the use of plasma image features led to better calibration performance. Their results further indicated that specific plasma image features were highly correlated with the plasma excitation state.

Zhang et al. [128] found that the oxide layer on the surface of T91 steel reduced the LIBS plasma temperature and increased the electron density. They used multiplicative scatter correction (MSC) to reduce interference caused by surface oxidation and applied K-fold support vector machine recursive feature elimination (K-SVM-RFE) to select the optimal spectral feature subset. A support vector machine (SVM)-based model for aging-grade evaluation was then established. After spectral correction, the accuracy of the validation set increased from 80.56% to 84.72%.

Lyu et al. [129] proposed a hybrid feature selection strategy that integrated expert knowledge—for example, pre-selecting 12 key spectral lines associated with major coal-ash elements such as magnesium, silicon, aluminum, calcium, and sodium—with data-driven algorithms, including Pearson correlation coefficient (PCC), mutual information (MI), least absolute shrinkage and selection operator (LASSO), and random forest (RF), to automatically identify important features. Experiments on three coal datasets demonstrated that this strategy achieved a lower root mean square error of prediction (RMSEP) than either purely expert-based or purely data-driven approaches.

## 5.2 Classification

Classification aims to identify or classify materials based on their spectral characteristics. The specific elemental composition patterns of different sample types are manifested in the spectrum as characteristic feature combinations. The classification model distinguishes and matches these combinations to determine the sample types. Only a brief overview of several representative classification paradigms is provided here; for more detailed reviews on LIBS classification, readers are referred to [130, 131].

Early LIBS classification studies mainly adopted traditional chemometric and machine-learning classifiers combined with manually selected spectral features. These methods, often characterized by transparent and interpretable modeling logic, have been widely applied in material identification and grade discrimination tasks. For example, Lu et al. [132] combined LIBS line intensities and intensity ratios with an SVM model to evaluate the aging grade of T91 heat-resistant steel. Zhang et al. [133, 134] applied partial least squares discriminant analysis (PLS-DA), principal component analysis–Mahalanobis distance (PCA-MD), linear discriminant analysis (LDA), and SVM to LIBS spectra of plant leaves, showing that traditional chemometric and machine-learning classifiers can achieve high accuracy in both leaf-type discrimination and small-area geographical origin tracing.

With the expansion of application scenarios, increasing attention has been paid to the robustness and generalization ability of LIBS classification models. Related studies typically focus on two levels: enhancing the model's ability to handle the intrinsic complexity of data and improving its adaptability to variations in external conditions (e.g. experimental conditions, sample matrices, instruments). Harefa et al. [135] applied nonlinear manifold-based dimensionality reduction techniques, including locally linear embedding (LLE), local tangent space alignment (LTSA), Laplacian eigenmaps (LE), and isometric mapping (Isomap), in combination with SVM classifiers to alleviate the curse of dimensionality in LIBS classification. Chen et al. [136] proposed a domain adaptation method based on Joint Distribution Adaptation (JDA) to reduce the distribution discrepancy between focused and defocused spectra, thereby mitigating the defocusing problem caused by surface fluctuations in aluminum alloy classification.

The introduction of artificial neural networks (ANNs) brought greater flexibility to LIBS classification, mainly through their ability to capture complex relationships among spectral variables. These studies marked a transition from conventional chemometric methods toward learning-based frameworks, and further paved the way for later deep-learning and data-fusion approaches. For example, Cui et al. [137] applied a multilayer perceptron (MLP) to wood species classification, while Wang et al. [138] further examined the robustness of MLP for plastics under varying conditions. Jamali et al. [139, 140] explored deep-learning-based rock classification by combining LIBS spectra with sample images, showing that appropriate fusion strategies—especially feature-level and advanced fusion—could further enhance classification performance.

## 5.3 Quantification

Quantitative analysis has been one of the central goals of LIBS since its invention, and it remains one of the most challenging aspects of LIBS data analysis. The complexity of plasma dynamics, the matrix effect, and other mechanisms make it difficult to establish a stable and universal relationship between the two. Therefore, developing reliable quantitative models has always been the key point of LIBS research. On the one hand, it is to optimize the analytical performance in specific application scenarios, and on the

other hand, it is to attempt to provide transferable model methods.

### 5.3.1 Physics-based model

Physics-based quantitative models rely on well-established physical principles and typically introduce simplifying assumptions to make the modeling tractable. The most conventional type of such models is the univariate model, which uses the intensity of a single spectral line to calibrate the analyte concentration based on the direct relationship between emission intensity and concentration. In this sense, the univariate model represents the simplest form of physics-based quantitative modeling. Its structural simplicity inherently limits its ability to capture the complex physical processes in LIBS and matrix effects. Compared with data-driven models, however, its key advantage lies in its full interpretability. Moreover, the generality of the underlying physical principles gives the model applicability across a wide range of matrices. As the understanding of LIBS plasma processes deepens—reflecting progress in fundamental research discussed in Section 3—it becomes possible to explicitly incorporate certain physical mechanisms into the quantitative model. This enables more accurate quantitative corrections while preserving model interpretability and generalizability.

Calibration-free LIBS (CF-LIBS) [141] can be regarded as a physics-based quantitative model. Its key advantage is that quantitative information can be obtained directly from the spectra without the need for calibration, although this comes at the cost of relying on stronger physical assumptions than calibration models. In practice, experimental conditions often deviate significantly from these ideal assumptions. The classical CF-LIBS method is based on several physical assumptions, including local thermodynamic equilibrium (LTE), optical thinness of the plasma, stoichiometric ablation, and plasma homogeneity. In recent years, studies on CF-LIBS have primarily focused on improving self-absorption correction, e.g., the work of Li et al. discussed in Section 3.1.2 [16]. Another example is the work of Yang et al. [142], who proposed a CF-LIBS method that automatically selects an internal reference line for each element, corrects its self-absorption, and employs particle swarm optimization (PSO) to improve plasma temperature estimation. Other assumptions of CF-LIBS, however, are more difficult to address systematically due to the complexity of the underlying physics. Given these limitations, CF-LIBS may be particularly suitable for scenarios where calibration is impractical or where high quantitative accuracy is not required.

One-point calibration LIBS (OPC-LIBS) [143] introduces a single-point calibration using one standard sample to compensate for deviations in CF-LIBS. Unlike the hybrid methods discussed later in Section 5.3.3, which integrate physical modeling with data-driven approaches, OPC-LIBS represents deviations from the underlying physical assumptions through a single empirical correction factor. Because this strategy does not introduce a data-driven modeling paradigm and relies on a lumped correction, its capacity to describe multiple plasma and matrix effects is inherently limited. As a result, the correction depends on matrix similarity and relatively stable experimental conditions. Under such conditions, OPC-LIBS may achieve satisfactory quantitative performance. Bai et al. [144, 145] applied OPC-LIBS to steel samples (Al–W–Mo coatings) in a vacuum environment ($5 \times 10^{-5}$ mbar), achieving relative errors below 1.64% for major elements and below 24.79% for minor elements. For samples with significantly different matrix compositions, Bai et al. [146] found that the applicability of OPC-LIBS depends on the concentration of the standard sample. They therefore proposed pre-classifying samples and using different reference points for quantitative analysis within different matrix ranges. Improvements to

OPC-LIBS proposed by Li et al. [147–149] avoid the direct use of transition probabilities, enabling the method to be applied to spectral lines with unknown atomic parameters.

### 5.3.2 Data-driven model

Data-driven models rely primarily on statistical-learning or machine-learning techniques to learn correlations between spectral features and target properties from data. Such methods emphasize predictive performance and flexibility, often without requiring explicit modeling of the underlying plasma physics. Compared with physics-based models, they generally offer greater flexibility in handling complex nonlinear relationships, but their interpretability and generalization may depend more strongly on the representativeness of the training data.

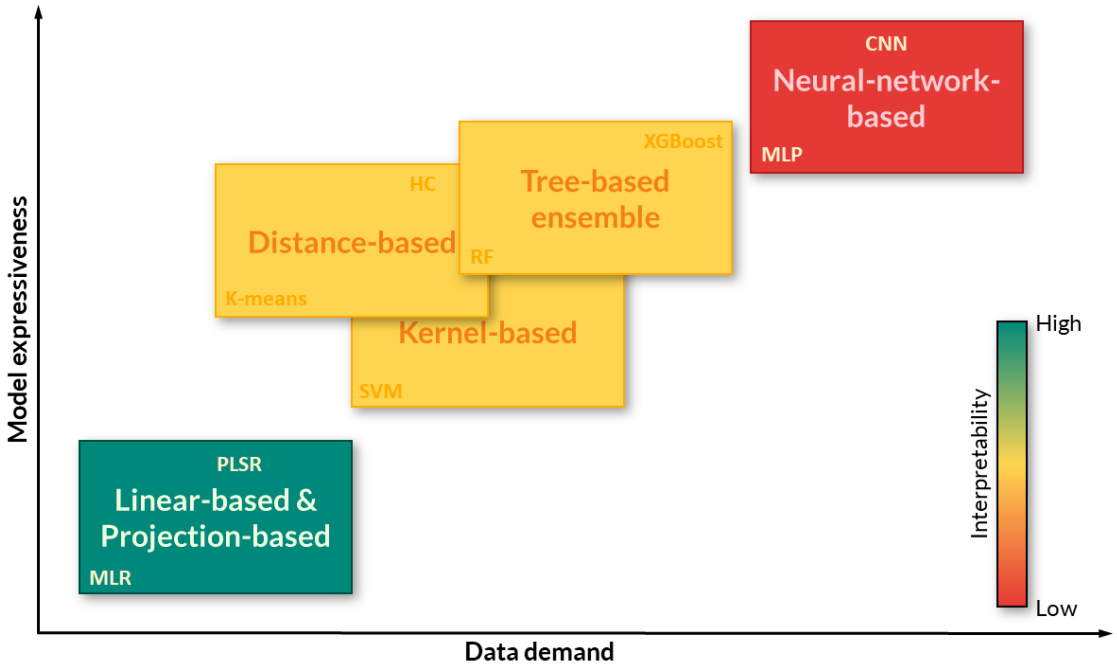


Figure 4: Landscape of data-driven models used in LIBS analysis. Here, model expressiveness qualitatively refers to the ability of a method to represent complex relationships in spectral data.

Data-driven methods used in LIBS span several representative algorithmic families. Fig. 4 provides a schematic landscape of these categories in terms of model expressiveness, data demand, and interpretability, while Table 4 summarizes their mechanisms, typical methods, and representative references. The figure is intended as a qualitative overview rather than a strict taxonomy, and the boundaries between categories are not absolute.

The early data-driven quantitative analysis in LIBS mainly employed linear or projection-based methods. These methods establish the relationship between spectral features and element concentrations through relatively simple structures and clear statistical assumptions, and usually have better robustness. In this line, efforts were devoted to improving variable representation and regression performance. Huang et al. [150] combined data-driven variable selection using principal component analysis (PCA) and canonical correlation analysis (CCA) with regression models including PLSR and support vector regression (SVR) for hardness prediction in aged T91 steel, and showed that the CCA-SVR combination achieved the best performance. Jiang et al. [151] applied kernel partial

Table 4: Representative data-driven methods for LIBS analysis.

| Method Category | Representative algorithms | Mechanism |
|---|---|---|
| Linear & projection-based | MLR, ridge regression, LASSO, PLSR, LW-PLSR, LDA, PLS-DA, PCR, PCA | Linear regression or latent-variable projection of variables |
| Kernel-based methods | SVM, SVR, K-ELM | Nonlinear mapping of spectral features via kernel functions |
| Distance-based methods | K-means, Hierarchical Clustering | Sample grouping based on pairwise distances, local neighborhood relations, or intrinsic geometric structure |
| Tree-based ensemble | RF, XG-Boost | Ensemble learning via recursive partitioning of the feature space |
| Neural-network-based | MLP, CNN | Data-driven nonlinear feature learning from spectral inputs |

least squares (KPLS) to biomass fuels with complex composition and pronounced matrix effects, showing that KPLS consistently outperformed linear PLS in predicting calorific value and proximate-analysis parameters.

Further developments also aimed to improve model robustness in situations where standard samples were limited or spectral interference was severe. Li et al. [152] developed a semi-supervised co-training regression method that expanded the effective training set by incorporating selected unlabeled samples, thereby significantly improving Cr prediction in high-alloy steels. In another study, Li et al. [153] employed selective ensemble learning to generate multiple regression learners and then combine a subset of diverse and accurate models for vanadium slag analysis, which improved the robustness of multi-component quantification in a highly interfered matrix.

To address performance degradation caused by variations in experimental conditions or sample matrices, and to extend the applicability of existing calibration knowledge, transfer learning and domain adaptation strategies have been explored in LIBS quantification. Chang et al. [154, 155] and Yang et al. [156] addressed the lack of high-temperature calibration samples by transferring room-temperature spectral information to high-temperature conditions through feature mapping, spectral conversion, or iterative weighting schemes, thereby improving Cr prediction accuracy. Ding et al. [157] aligned pellet and atmospheric particle spectra for particulate matter analysis, while Dong et al. [158] transferred calibration knowledge from coal pellets to coal powder flow for online coal-property prediction.

### 5.3.3 Hybrid model

Hybrid models introduce data-driven approaches on the basis of physics-based models to capture complex nonlinear effects, or incorporate physical constraints within the data-driven frameworks to enhance interpretability and model robustness. Compared with physics-based models, they possess greater model complexity to represent complex physical effects, particularly matrix effects. Compared with data-driven models, they are grounded in physical principles, which may enable them to learn more physically meaningful features, thereby reducing the risk of overfitting to spectral noise or other

Table 5: Comparison of modeling approaches in LIBS.

| Dimension | Physics-based models | Data-driven models | Hybrid models |
|---|---|---|---|
| Modeling principle | Explicit physical mechanisms | Statistical relationships learned from data | Combination of physical knowledge and data-driven learning |
| Interpretability | High | Limited | Moderate to high |
| Generalization behavior | Depends on validity of physical assumptions | Depends on representativeness and size of training data | May provide improved robustness across matrices, especially with limited training data |
| Representative methods | CF-LIBS | PLS, SVR, MLP | DF-PLS, SKR |

non-physical features. This can improve their generalization across different matrices and enhance long-term model stability.

The dominant factor based PLS method proposed by Wang et al. [159–163] represents a typical hybrid model. The method first constructs a dominant-factor relationship using characteristic spectral lines with clear physical significance to explain most of the concentration variation. PLS is then introduced to utilize full-spectrum information to model the residuals not explained by the dominant factors. In this way, matrix effects and other complex plasma-related effects are modeled while maintaining physical consistency and reducing the risk of overfitting.

The dominant-factor concept can also be integrated with more complex machine learning models. Song et al. [164] proposed dominant factor support vector regression (DF-SVR) and dominant factor kernel extreme learning machine (DF-K-ELM), which use SVR and K-ELM to model the residuals of the dominant factors. Across ten quantitative tasks in a coal analysis dataset, DF-K-ELM achieved the best performance in four tasks and obtained the highest average rank.

The aforementioned methods can be viewed as introducing data-driven approaches into physics-based models to enhance model performance. Song et al. [165, 166] also proposed hybrid methods in the opposite direction by incorporating physical constraints into data-driven models. Spectral knowledge regression (SKR) directly incorporates the linear relationships of physically meaningful variables into the objective function, thereby improving quantitative accuracy while maintaining interpretability. In industrial online coal quality analysis, the analytical results for calorific value, sulfur content, and volatile matter met the requirements of national standards.

As shown in Table 5, physics-based models provide strong interpretability but may be constrained by simplified physical assumptions, whereas data-driven models offer greater flexibility but rely more heavily on the representativeness of training data. Hybrid models attempt to balance these two aspects by integrating physical knowledge with data-driven learning.

## 5.4 Multimodal modeling

As discussed in Section 4.3, the development of spectral tandem technology enables the acquisition of complementary information from multiple modalities. Effectively utilizing these multimodal signals requires corresponding modeling strategies. A schematic overview of the main modeling paradigms is provided in Fig. 5.

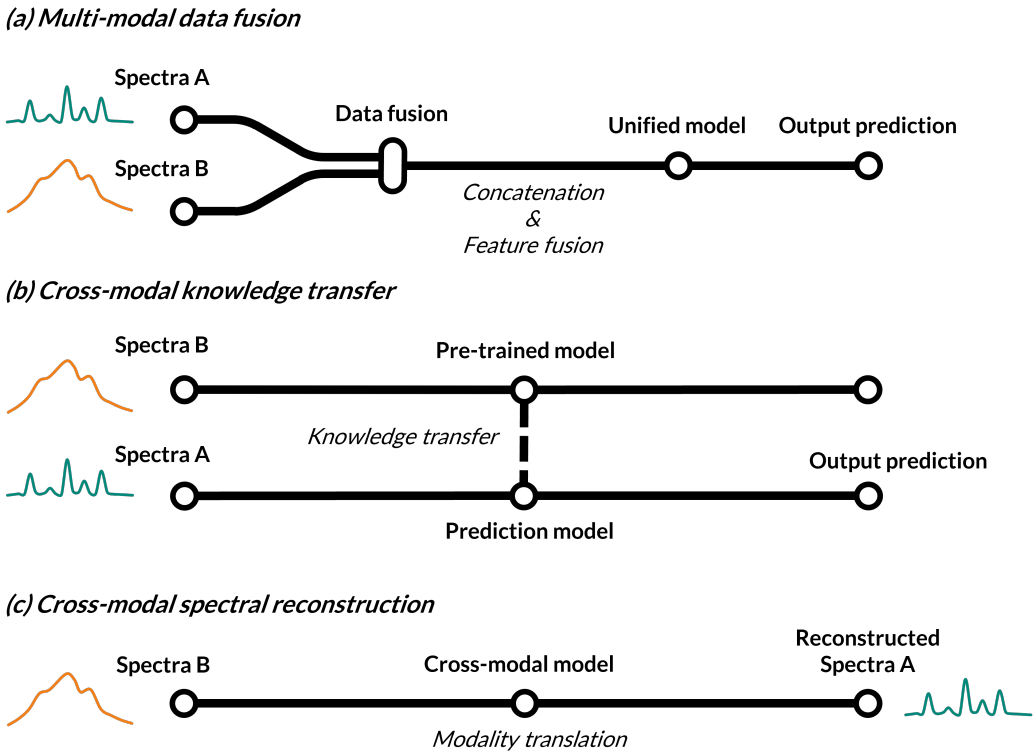


Figure 5: Paradigms of multimodal modeling in spectroscopic analysis.

Data fusion has been the most common multimodal modeling paradigm in LIBS-based tandem systems, in which information from different modalities is jointly exploited for the same analytical task. According to the stage at which information is integrated, data fusion can be categorized into data-level (low-level), feature-level (mid-level), and decision-level (high-level) fusion [167–169]. In the currently reported LIBS-based tandem studies, fusion has been implemented mainly at the data and feature levels. Data-level fusion usually involves directly concatenating the preprocessed spectra from different modalities and using the combined data as the input to a single model. Representative examples of data-level fusion include LIBS–Fourier transform infrared spectroscopy (FTIR) fusion for coal analysis [170] and LIBS-Raman fusion for bacterial classification [171]. Feature-level fusion has been more commonly explored in recent studies, where informative variables are first extracted from each modality and then combined for downstream modeling. Early examples include LIBS-Raman fusion based on selected discriminative variables [172]. More recently, Zhao et al. [173] compared data-level and feature-level fusion within the same LIBS-NIRS framework, showing that feature-level fusion outperformed direct concatenation in their heavy-metal quantification task. Zhang et al. [174] developed a dual-branch attention-based convolutional neural network for LIBS-NIRS analysis, in which the two modalities were first processed in separate branches for deep feature extraction and then fused under attention-guided weighting. This moves

feature-level fusion from manual or shallow variable combination toward end-to-end deep cross-modal feature learning. Besides the three conventional categories, Yao et al. [175] proposed a stepwise hybrid model in which ash and moisture were first predicted from LIBS and NIRS, respectively, and then incorporated together with fused LIBS-NIRS data to determine calorific value and volatile matter.

Beyond data fusion, recent studies have also begun to explore cross-modal knowledge transfer, in which one modality is used not together with, but in support of, another modality. Song et al. [176] proposed a spectral feature distillation strategy in a LIBS-NIRS system. In their framework, a high-performance LIBS-based model serves as the teacher, while an NIRS-based model acts as the student, so that refined spectral knowledge learned from LIBS can be transferred to improve the quantitative accuracy of portable NIRS while preserving its cost-efficiency and field-deployment advantages. In another study, Song et al. [177] extended this idea to a LIBS-enhanced smartphone video imaging (LE-SVI) strategy, in which LIBS-derived elemental fingerprints were used as chemical references to guide the SVI model. Through spatial matching between LIBS ablation spots and SVI pixels, the paired data were used to transfer LIBS spectral knowledge into the imaging modality, enabling elemental quantification and mapping using only smartphone videos during inference. These strategies shift the role of the auxiliary modality from joint input to transferable knowledge. Conversely, the same paradigm could also be conceptually extended to scenarios where structurally or chemically informative modalities are used to guide LIBS representation learning and thereby improve LIBS-based modeling. It should be noted that cross-modal knowledge transfer does not introduce fundamentally new spectral information into the receiving modality, since the model still operates on a single-modality input. Instead, it encourages the model to exploit its own spectral information in a way that is more closely aligned with the representations learned from the source modality. Its effectiveness in improving performance lies in the fact that the alignment is constrained by a specific downstream task.

Another possible form of cross-modal learning is cross-modal spectral reconstruction, where one spectral modality is used to generate or infer another. In the broader spectroscopy literature, Neo et al. [178] developed Spectral Conversion Autoencoders to convert among FTIR, Raman, and LIBS spectra for the same sample, thereby enabling synthetic spectral generation across modalities. They further combined the reconstructed Raman and LIBS spectra with real FTIR spectra for downstream plastic classification, relying on only an FTIR sensor in practical deployment. From a LIBS-based perspective, such a workflow suggests two directions: LIBS as the source spectrum or the reconstructed spectrum, enhancing LIBS-based analysis or other modality-based systems, respectively. In this sense, reconstruction-based approaches become functionally close to knowledge transfer, since the reconstructed spectra are ultimately used for downstream modeling, and this makes the workflow effectively equivalent to one that takes LIBS spectra as input and outputs analytical results, except that it has an intermediate representation, namely the reconstructed spectra. In addition, LIBS spectra reconstructed from other modalities may also be used to refine or augment real LIBS spectra, in turn supporting LIBS-based modeling by expanding training data or improving measured LIBS spectra under noisy, incomplete, or otherwise constrained conditions.

To ensure that the models truly exploit multimodal information rather than merely learning accidental correlations, comparative validation should be conducted for the above paradigms. For data fusion and cross-modal knowledge transfer, such validation should include comparisons with models in which the auxiliary modalities are removed. When

possible, the contribution of features should also be examined to confirm that the improvement originates from physically meaningful complementary information. For spectral reconstruction, validation should include not only downstream prediction accuracy, but also the physical interpretability of the reconstructed spectra, such as the presence of characteristic peaks with chemical significance.

# 6 Applications

Ultimately, the value of LIBS is reflected in its ability to address real analytical tasks under practical constraints. This section mainly addresses the third core problem, namely how reliable analytical performance can be maintained under practical deployment constraints. Specifically, it examines how scenario-specific requirements and deployment constraints shape the entire analytical process of LIBS. At the same time, application studies provide a comprehensive test of the preceding two problems, because the control of the plasma signal source, the acquisition of raw signals, and the transformation of those signals into reliable analytical results must all be achieved together under real operating conditions. From this perspective, the following sections review the progress of LIBS in representative application fields in China, including coal analysis, metallurgy and mineral processing, marine exploration, and nuclear fusion applications, and discuss how practical demands have, in turn, driven the further development of the technique.

To make this connection explicit, Fig. 6 revisits the problem-oriented framework proposed in Section 2 from an application-oriented perspective. Compared with Table 1, this figure further provides a qualitative assessment of the extent to which these problems have been explored in the studies reviewed in this article. The assessment is not intended as a strict bibliometric ranking, but as a synthetic judgment based on the representative literature discussed above. Problems that have been extensively investigated or for which relatively stable mechanistic or methodological explanations have been established are distinguished from those that have only been partially explored or remain largely underexplored. In this way, the figure serves as a bridge between the problem-oriented framework and the following application-oriented review, clarifying which aspects of the analytical chain have provided mature support for practical applications and which aspects still constitute major bottlenecks for reliable deployment.

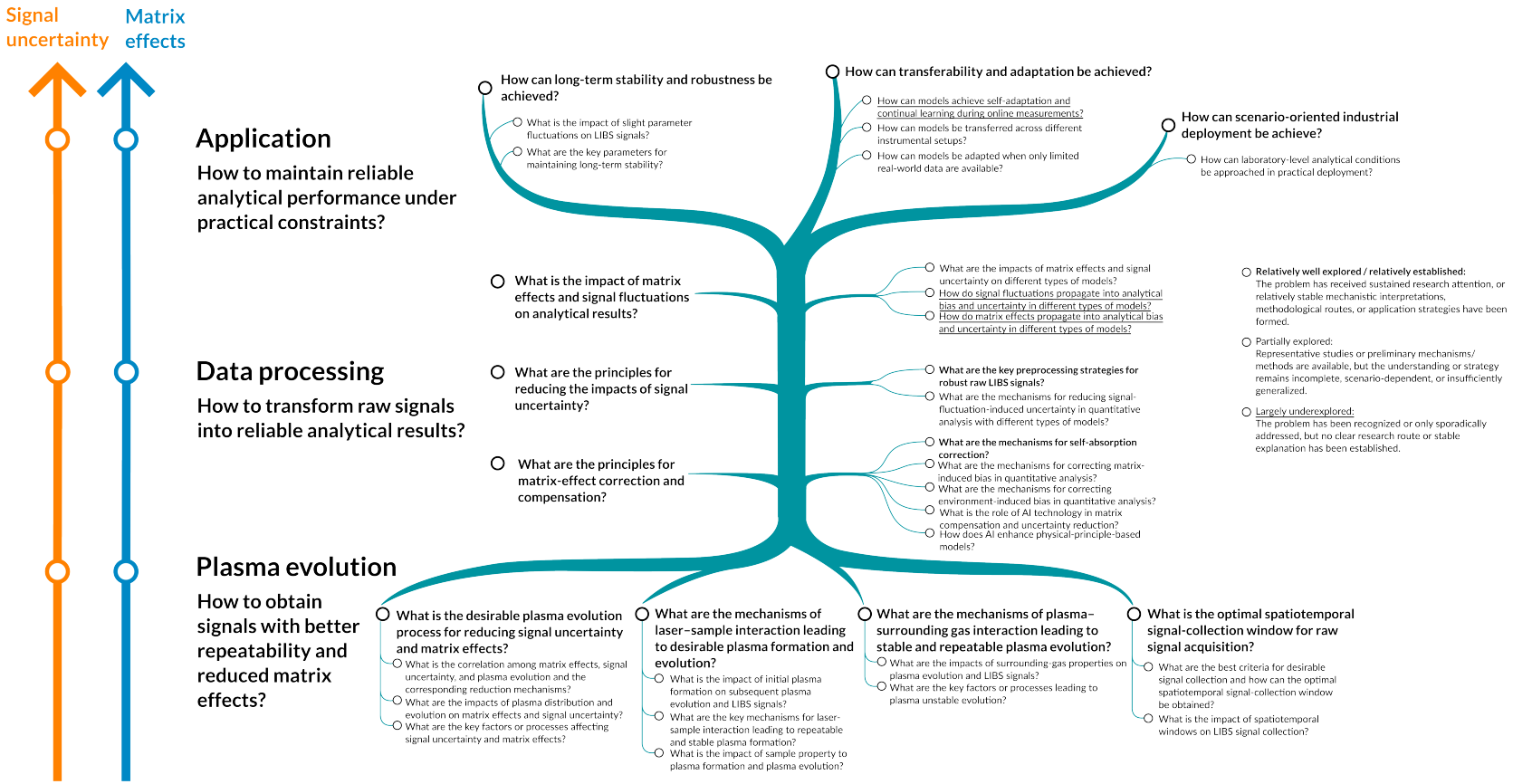


Figure 6: Problem-oriented map of the LIBS analytical chain and its current exploration status.

## 6.1 Coal analysis

As China's energy system transitions toward a low-carbon and more flexible structure, the efficient and clean utilization of coal remains an important issue. Coal analysis provides the technical basis for coal pricing, blending, and combustion optimization, and is therefore of increasing importance. Coal quality parameters typically include proximate analysis (moisture, volatile matter, ash, and fixed carbon), ultimate analysis (C, H, O, N, and S), calorific value, and other parameters such as ash fusion temperature and Hardgrove grindability index. For power plants and coal processing facilities, the key requirement of coal analysis is rapid, online, and representative measurement under industrial conditions.

The advantages of LIBS, including rapid simultaneous multi-element analysis and minimal sample preparation, make coal analysis a typical application scenario for the technique in industrial settings. However, coal analysis also exemplifies the major challenges faced by LIBS in practical applications: the complex coal matrix, sample heterogeneity, and harsh industrial environments significantly affect quantitative analysis. An effective online coal analysis method should satisfy all the following metrics: precision, i.e., repeatability between samples or between successive laser pulses on the same sample; accuracy, i.e., the closeness of the result to the reference value; representativeness, i.e., the ability of the measurement to reflect the average composition of the coal feed; and long-term stability, i.e., the ability to maintain reproducible results over extended operation.

Ensuring a relatively stable and comparable plasma is a prerequisite for any meaningful quantitative analysis. It guarantees measurement precision, thereby creating room for the model to further improve accuracy. In industrial environments, splashing fly ash can disturb plasma stability and contaminate optical components. Therefore, negative-pressure extraction or gas-flow purging is commonly adopted to mitigate these effects [179]. The complex composition of coal leads to particularly severe matrix effects. Moisture content [13] and volatile matter [32, 180, 181] directly influence the laser–matter interaction and the subsequent plasma evolution. For a given coal type, the volatile matter content usually varies within a limited range, allowing its effect to be partially captured by the calibration model. In contrast, raw coal often exhibits highly non-uniform internal and surface moisture distributions [182]. Under in-situ measurement conditions, the moisture content used as an industrial index may not accurately represent the local moisture content at the measurement point. Therefore, to ensure measurement repeatability, grinding and drying pretreatment of coal samples are generally necessary steps. From the perspective of physical matrix effects, the particle size of coal also influences plasma evolution [183, 184]. A practical strategy involves pressing the ground and dried coal powder into pellets to ensure consistent surface conditions. In addition, previously mentioned plasma modulation approaches—such as spatial confinement [42, 185, 186] and surface enhancement [187]—have also been applied to coal analysis to improve plasma stability and signal reproducibility.

The heterogeneity of coal poses a challenge to the representativeness of online analysis. The spectrum from a single laser pulse only reflects the local composition at the ablation spot and may fail to represent the average properties of the coal feed, especially for blended coal feeds in settings such as thermal power plants. Therefore, achieving physical homogenization through grinding, blending, and pellet pressing is generally considered the most direct physical approach for overall characterization. Alternatively, Yao et al. [93, 94, 188–191] and Dong et al. [158, 192, 193] have explored strategies for direct de-

tection of particle flows. In practice, most particle-flow systems still rely on pre-grinding and do not completely eliminate pre-treatment steps. They employ statistical criteria based on spectra [188, 189] or auxiliary images [193] to screen spectra, aiming to eliminate outliers and improve prediction stability. These methods can effectively enhance the consistency of predictions. However, the plasma corresponding to the screened spectra may not necessarily be representative of the whole. In highly fluctuating particle systems, these screening criteria themselves may introduce potential selection bias; therefore, statistical consistency does not necessarily guarantee compositional representativeness.

The matrix effects of coal also manifest in the complex spectra arising from its diverse elemental composition. An effective quantitative model should extract key information from these spectra while maintaining robustness against both short-term fluctuations and long-term drift. The dominant factor based PLS model developed by Wang et al., as mentioned in Section 5.3.3 [159–162], employs physically meaningful spectral lines as dominant factors to ensure quantitative robustness, while integrating the modeling capability of data-driven methods to capture the complex spectral features of coal. Building on this framework, they also developed an adaptive database method [163]. For a measured spectrum that, after spectral standardization, exceeds a similarity threshold with spectra in the database, the corresponding composition is directly retrieved. For new samples, the dominant factor based PLS model is used for quantification, and the results are then added to the database. This strategy allows the model to adapt to plasma fluctuations at the model level, thereby providing consistent quantitative results.

Compared with elemental analysis, applying LIBS to coal proximate analysis and calorific value prediction presents an additional challenge. LIBS measures emission from atoms and ions in the plasma, which is generally strongly correlated with elemental concentration, despite issues such as non-stoichiometric ablation and plasma inhomogeneity. However, an inherent scale mismatch arises when relating this emission information to industrial indicators such as volatile matter or calorific value. In other words, the relationship between such emission information and these industrial indicators inherently depends on the properties of the coal matrix, and may become unreliable when environmental conditions change or coal types vary. One strategy is to introduce tandem techniques, utilizing other spectroscopic methods to acquire molecular-level information to complement the elemental information provided by LIBS. Yao et al. [170, 194] developed data fusion methods combining LIBS with infrared spectroscopy, achieving improved performance in predicting proximate analysis parameters and calorific value. Another direction is to establish separate quantitative models for different matrix types, following a classification-then-quantification strategy known as matrix matching. Gu et al. [195] applied matrix matching to coal analysis, improving several quantitative performance metrics.

In practical industrial environments, instrumentation and on-site conditions often struggle to maintain stability over extended operational periods. Frequent manual calibration of instruments is generally impractical in industrial settings. The long-term repeatability of quantitative results therefore depends on effective environmental control during measurement and on the transferability of quantitative models, or on the instrument's built-in self-calibration capability. Li et al. [179] proposed a closed-loop feedback method to stabilize laser energy. In a month-long test, the RSD of laser energy was reduced from $\pm 5.2\%$ to $\pm 1.3\%$.

In a review, Sheta et al. [182] classified online coal analysis into inline and at-line modes. Inline analysis directly examines the coal flow on the conveyor belt in a coal

plant and essentially represents in-situ measurement. At-line analysis involves automatic sampling from the conveyor belt, followed by automated sample preparation and analysis. Sample preparation typically includes grinding, homogenization, drying, and pellet pressing. In industrial scenarios with high precision requirements, at-line analysis can be regarded as a currently viable approach for LIBS-based coal analysis, as it improves plasma repeatability [196, 197]. An at-line coal analysis system developed by Wang et al. maintained quantitative performance meeting national standard requirements over a 6–7 month operational period. This demonstrates the feasibility of long-term precise quantification in the at-line sampling mode for bituminous coal on an air-dried basis, providing a representative example of LIBS application in industrial online analysis. Furthermore, industrial experience suggests that many coal quality indicators correlate strongly with carbon content. If carbon content can be determined with sufficient precision and accuracy, it may serve as an anchoring variable linking LIBS spectra to macroscopic indicators. This idea does not ignore matrix dependence but rather seeks to reduce the dimensionality of the problem and potentially improve stability within specific coal categories.

Technological advancements in LIBS for coal analysis have largely relied on the integration of engineering controls, sampling strategies, and modeling methods. Future developments may arise from a deeper understanding of the intrinsic properties of coal and the underlying physics of LIBS, as well as from the incorporation of additional information dimensions.

## 6.2 Metallurgy and mineral processing

Metallurgy and mineral processing are key stages in mineral resource utilization and form a cornerstone of the modern industrial system. Conventional analytical methods used in metallurgy are typically offline, including atomic absorption spectroscopy (AAS), inductively coupled plasma optical emission spectroscopy (ICP-OES) and XRF. With increasing digitization and continuous processing in metallurgical production, LIBS has attracted extensive attention owing to its advantages for real-time analysis. According to the physical state of materials, the main applications of LIBS in metallurgy and mineral processing include the analysis of solid alloys, molten metals, and ore slurries.

The rapid analysis speed and minimal sample preparation requirements of LIBS make it attractive for fast compositional analysis and identification of solid metal alloys. Beyond this application itself, advances in offline metal analysis also contribute to a better understanding of metal matrix effects, which is beneficial for online applications. In addition to plasma-side matrix effects, such as the distillation effect arising from differences in melting and boiling points of elements [198], surface roughness [199], and reflectivity [11], a major spectral characteristic is the presence of numerous emission lines and severe spectral interferences. Consequently, relatively complex models are typically required to account for these matrix effects. He et al. [200–206] combined femtosecond LIBS (fs-LIBS) with spark discharge and optimized modeling methods, achieving industrial-level quantification and classification for alloys such as steel, aluminum, and magnesium. Sun et al. [122, 123, 207, 208] explored various modeling approaches, including ANN and PCA, together with data correction strategies for alloy quantification and classification. It should be noted that although increasing model complexity can improve performance on complex matrices compared with linear models, it may also limit generalization across a broader range of matrices. This occurs because models tend to overlearn correlations specific to the training set that arise from material properties rather than reflecting in-

trinsic element–spectrum relationships. In principle, genuine matrix effects and such spurious correlations are not inherently coupled. Therefore, the reliability of complex models should be evaluated using validation strategies that deliberately test matrix generalization, rather than relying only on random train–test splits. For example, validation can be performed across different matrix groups, sample batches, instruments, or measurement periods.

In steelmaking and non-ferrous metallurgical processes, real-time analysis is critical for process control and optimization. LIBS is currently one of the few analytical techniques capable of operating under such extreme conditions, characterized by high temperatures, intense thermal radiation, and metal vapors. However, these harsh environments also pose significant challenges for LIBS measurements, as they strongly influence the plasma state and the emission process [209]. As briefly mentioned in Section 4.2, Sun et al. [90, 91, 210] developed a series of integrated solutions for the online analysis of molten metals based on a Cassegrain telescope and double-pulse LIBS (DP-LIBS), which have been validated in industrial environments. Zeng et al. [211, 212] developed a combined LIBS–NIRS system for the simultaneous measurement of melt temperature and elemental composition, demonstrating its effectiveness for carbon steel melts.

Mineral processing is a preliminary stage in the metallurgical value chain. Grade analysis typically involves time-consuming sampling and subsequent laboratory analysis. XRF, one of the most widely used online techniques in mineral processing, is limited in its ability to detect light elements. LIBS offers a promising alternative due to its capability for rapid multi-element detection, including light elements. Sun et al. [213–217] developed SIA-LIBSlurry, China's first LIBS-based online slurry grade analyzer, which has been successfully deployed and operated in phosphate and iron ore processing plants. Furthermore, to address long-term stability and precision issues encountered during practical operation, they developed corresponding calibration and modeling strategies based on operational data.

Beyond the three major application scenarios discussed above, researchers have also explored LIBS for other stages across the metallurgical process chain. Yang et al. [218–220] investigated the measurement of sinter basicity using various quantitative models. To address metal segregation and inclusion issues, Wang et al. [10, 221–223] performed micro-area analysis of metal surfaces using surface mapping based on ps-LIBS. Li et al. [224] further developed a three-dimensional spatially resolved analysis system based on ps-LIBS. Deng et al. [225] employed DP-LIBS to determine trace elements in rare-earth ores, while Ji et al. [61, 121, 226] developed plasma modulation and spectral standardization strategies to address the challenges of complex matrices and low concentrations in uranium ore quantification. Ji et al. [227] further developed a severely overlapped-spectra decomposition approach for the spectral interference in uranium ore. These studies demonstrate the flexibility of LIBS in addressing diverse analytical tasks in metallurgy and mineral processing. Although many of these applications remain at the laboratory stage, they collectively indicate the broad potential of LIBS in this field.

## 6.3 Marine exploration

With the rapid development of measurement technology and vehicle platforms such as manned submersibles and remotely operated vehicles (ROV), there is a critical need for in-situ chemical sensors for ocean exploration. LIBS is an attractive technique for the in-situ analysis of seawater and submerged solid objects, due to its rapid, multi-elemental

and standoff analysis capabilities. Over the past ten years, several underwater LIBS instruments have been successfully developed and deployed for deep-sea applications [228–232]. Recently, more attention has been paid to the in-situ analysis of deep-sea mineral deposits, such as manganese nodules, seafloor massive sulfides, and ferromanganese crusts, which are considered a new frontier for mineral exploration and extraction [233].

In 2015, the University of Tokyo reported a deep-sea LIBS system named ChemiCam and successfully analyzed seawater and mineral deposits at a depth of over 1000 m [228]. They realized an in-situ quantitative analysis of deep-sea minerals in the hydrothermal vents area [229]. In 2017, the Ocean University of China reported a 4000 m rated deep-sea LIBS system named LIBSea and obtained the spectral profiles of seawater at depths over 1800 m [229]. The LIBSea system was deployed by the ROV Faxian and in June 2015 was successfully applied for hydrothermal field measurements at the Manus area. Subsequently, a more compact system named LIBSea II was developed which is capable of in-situ analysis of submerged solids at depths up to 5000 m [231]. In 2019, the LIBSea II system was deployed on a ROV Haima for deep-sea trial, and atomic lines of K, Na, Ca and molecular bands of CaOH from a carbonate rock sample were obtained at depths of 1400 m. In 2020, the Ocean University of China reported a depth profiling investigation of seawater using combined Raman and LIBS techniques [232]. The hyphenated system consists of two independent Raman and LIBS spectrometers, and depth profiles of multiple ocean parameters were extracted from the Raman and LIBS spectra with a maximum depth of 1800 m and a resolution of 1 m. Recently, a high-sensitivity micro-gas column assisted LIBS system (MGC-LIBSea) was developed and the feasibility was tested nearshore at a depth of 18 m [234]. A deep-sea long-pulse LIBS system (iLIBSea) was also developed with integrated microscopic imaging capability, and the spectra of Cu target were obtained under simulated 50 MPa pressure conditions [235].

Driven by the LIBS applications in deep-sea, great efforts have been made in the laboratory to reveal the characteristics of LIP in water [236–238] and especially the high-pressure impacts on underwater LIBS signals [239–242]. Tian et al. [236] studied the spatiotemporal characteristics of Ca ionic, atomic, and molecular emissions from underwater plasma which gives new ideas to improve the analytical performance of underwater LIBS by using molecular emissions. They built a high-pressure chamber with a maximum pressure of 50 MPa (corresponding to the ocean depth of 5000 m) to study the pressure effects. It showed that at high pressures, strong plasma-bubble interaction occurs at the late stage of plasma evolution and the bubble dynamics at high pressures play a key role in the characterization of plasma emission [239]. A properly enhanced pressure (10-30 MPa) is beneficial for improving the underwater LIBS signals that both higher spectral intensity and longer persistence of the plasma emission can be achieved [240].

Compared with the LIBS measurements in gases, the underwater LIBS spectrum is characterized by strong continuum radiation and quite weak spectral features. This is due to the incompressible nature of water, where the underwater plasma suffers strong quenching and confinement effects, with low temperature, high density and short emission lifetime [243]. To overcome these problems, many efforts have been devoted to the improvement of laser irradiation schemes such as using double-pulse [244–246] or long-pulse lasers [247, 248]. Tian et al. demonstrated the important role of laser focusing geometry including the spherical aberrations and focusing angles on the reduction of pulse-to-pulse fluctuations, for LIBS analysis in bulk water [249, 250] and on submerged solid target [251]. Spectrum normalization methods were also developed by using the plasma acoustic signals [252, 253] or plasma emission images [254] as external references that can improve

the stability and quantitative performance of underwater LIBS. Recently, Lu et al. [255] proposed an effective signal-enhancement strategy for deep-sea LIBS by draining the water from the sample surface with high-pressure helium gas, which allowed the plasma excitation environment to be converted from high-pressure water to high-pressure gas. They [256] further developed an elemental chemical sensor system based on this method. Nitrogen was selected as the high-pressure working gas, and LIBS spectra of carbon steel samples were successfully acquired at a depth of 6000.8 m underwater, reportedly for the first time. Sun et al. [257] developed a gas-flow fiber-optic LIBS probe for underwater environments, and the trace chromium in steel target was quantitatively analyzed with a detection limit of 95 mg/kg.

Further work is still needed to enable the practical use of LIBS in deep-sea exploration. The sensitivity of underwater LIBS at high pressures needs to be improved, in conjunction with deeper understandings of the laser ablation mechanisms in water. Advanced algorithms for data processing such as using machine-learning or deep-learning methods would be useful to improve the analytical performance of LIBS especially in complex deep-sea environments. Underwater LIBS instruments should be further downsized and made more intelligent, with autofocus capabilities that allow easier operation by underwater vehicle manipulators.

## 6.4 Nuclear fusion applications

A review of LIBS application in nuclear fusion technology was published in 2016 by Ding's group [258]. This paper emphasizes some significant recent advancements in the application of LIBS within nuclear fusion devices. Li et al. [259] investigated the fuel (deuterium) retention behavior in the EAST device using an in-situ LIBS system. Their results show that the amount of deuterium (D) retention increases as the local edge D particle fluence rises. This study addressed the research gap regarding the correlation between fuel retention and edge plasma conditions during long-pulse plasma operations in EAST. Liu et al. [260] investigated Lithium (Li)-H/D co-deposition under Li-wall conditions in EAST using an in-situ LIBS system. The study found that the LIBS technique can assess the degree of redeposition on the first wall. Li-wall conditioning significantly reduces the $H/(H^+D)$ ratio in the vacuum vessel due to the strong H/D adsorption capability of Li. Hu et al. [261] developed laser-induced ablation spectroscopy (LIAS) combined with LIBS to evaluate static and dynamic fuel retention on the first wall without removing tiles between or during plasma discharges in EAST.

LIBS has been used to study plasma-facing components in laboratory conditions, providing valuable insights into elemental distribution for research on plasma-wall interactions. Hai et al. [262] demonstrated the capability of collinear DP-LIBS under vacuum conditions. For an exposed divertor tile of EAST tokamak, significant increases in the emission line intensities of various minor elements (such as Mo, Si, Fe, Cr, Ti, Ni and Ca) were observed in DP-LIBS, while no spectral signal was obtained in single-pulse LIBS (SP-LIBS). Hai et al. [262] used DP-LIBS for the online measurement of the laser ablation process of the ultrathin co-deposition layer on the first mirrors of HL-2A tokamak during cleaning. The real-time monitoring and accurate identification of the interface boundary can provide important information regarding the cleaned mirror surface to avoid undercleaning. Li et al. [263] studied the distribution of D retention in the Li-D co-deposition layer on EAST divertor tiles. The depth profile behaviors of Li and D suggest that D retention in the divertor tiles resulted from Li–D codeposition processes during D discharge

in EAST. Imran et al. [264] used LIBS for depth-resolved identification of impurities deposited on the EAST divertor tile. The study shows that LIBS has the potential to monitor the erosion and deposition of PFCs in fusion devices. Hu et al. [265, 266] studied the characterization of impurities deposited on W divertors, the Mo first wall, and the graphite main guard limiter from EAST using a portable LIBS system. The CF-LIBS method was used to determine the relative content of impurities on the PFCs. The quantitative results of the impurities deposited on PFCs further provide a more detailed understanding of the variations in impurity deposition. Liu et al. [267] quantitatively investigated the impurity deposition layer on the graphite tile removed from the dome region of the HL-2A tokamak lower divertor using the ex-situ LIBS approach.

Researchers from Ding's group and his collaborators are also making contributions to the application of LIBS on international nuclear fusion devices, including the largest stellarator in Germany and the superconducting tokamak KSTAR in Korea. For example, Li et al. [268] analyzed graphite tiles from the Wendelstein 7-X stellarator that were exposed to helium and hydrogen plasma using picosecond LIBS (ps-LIBS). They investigated depth profiles of each element and a 2D profile of the H/C atom ratio on the surface. Additionally, Li et al. [269] used ps-LIBS combined with laser-induced ablation quadrupole mass spectrometry to study the elemental depth distribution and fuel retention on PFCs from the divertor baffle of W7-X. These studies effectively demonstrate the ability to determine element-resolved layer thicknesses and hydrogen retention in PFCs exposed in W7-X. Another example is Sun et al. [270] who used LIBS to measure deuterium retention and carbon deposition on the surface of castellated blocks from the KSTAR. The analysis of C, D, and Be deposition on different-shaped blocks provided valuable insights for theoretical models on plasma-wall interaction.

Recently, Ding and co-workers [271] have made significant progress in the quantitative analysis of D and He retention in high-$Z$ wall materials such as tungsten (W) and molybdenum (Mo), using LIBS combined with laser-induced desorption quadrupole mass spectrometry (LID-QMS) for calibration. The developed method was successfully applied to the quantitative determination of D and He in complex deposited layers extracted from an actual HL-2A tokamak marker tile. In W/Mo mixed deposition layers, the LIBS detection limit for D was approximately 0.24 at.%, corresponding to an areal density of $2 \times 10^{14}$ D $\cdot$ mm$^{-2}$. For He, the LIBS detection limit reached 0.14 at.%, with an areal density limit of $\sim 1.2 \times 10^{14}$ He $\cdot$ mm$^{-2}$, verifying that the method enables trace He analysis in high-$Z$ materials with average relative errors of 8.0% for D concentration and 26.0% for He. The LIBS/LID-QMS combined approach demonstrates strong applicability and reliable quantification for D/He retention in complex deposited layers under realistic tokamak conditions.

## 6.5 Other applications

In addition to the major application fields discussed above, LIBS has also been explored in a wide range of other scenarios. Although these applications differ substantially in target materials, operating environments, and analytical objectives, they share a common motivation: to exploit the unique strengths of LIBS. At the same time, each application domain poses its own challenges. Rather than reviewing each topic in detail, this section provides a concise overview of these representative domains from the perspectives of target analytes, key challenges, LIBS-specific advantages, deployment modes, and current research focuses, as summarized in Table 6.

Table 6: Overview of representative LIBS application domains.

| Application domain | Analytical targets | Key challenges | LIBS-specific advantages | Typical deployment mode | Representative research focus | Ref. |
|---|---|---|---|---|---|---|
| Coal analysis | proximate analysis parameters, ultimate analysis parameters, calorific value, other coal properties | Matrix effects, representativeness, long-term stability | Rapid multi-parameter analysis with minimal preparation | Inline / at-line | Industrial index prediction, matrix matching, data fusion | [93, 97, 179, 183, 188, 189, 192, 193, 272–278] |
| Metallurgy and mineral processing | Major and trace elements, grade-related parameters | Complex matrices, high-temperature operation | Rapid multi-element analysis for process monitoring | In situ / online / standoff | Alloy quantification, molten metal LIBS, slurry grade analysis | [95, 200–206, 218–220, 225, 279–281] |
| Marine exploration | Elemental composition of seawater and submerged solids | High-pressure liquid environments, fast plasma cooling | Rapid multi-element analysis in underwater environments | In situ / submersible-based | Underwater LIBS systems, high-pressure signal enhancement | [230–252, 255, 257, 282, 283] |
| Nuclear applications | Fuel retention, impurity deposition, and PFC surfaces | Harsh device environments, thin deposited layers | In-situ analysis of hazardous and inaccessible surfaces | In situ / laboratory | Fuel retention analysis, PFC depth profiling | [258, 259, 261–263, 265–270, 284, 285] |
| Atmospheric analysis | Atmospheric particles, gaseous species, and trace elements | Low concentration, transient signals | Real-time in-situ atmospheric sensing | In situ / online | Aerosol LIBS, transfer learning, atmospheric carbon detection | [286–291] |
| Biomass analysis | Alkali metals and biomass fuel properties | Matrix effects, sample heterogeneity | Rapid multi-parameter analysis with minimal preparation | Laboratory / at-line | Matrix-effect correction, normalization, multi-property prediction | [292–294] |
| Biomedicine | Tissues, biofluids, microorganisms, and pharmaceuticals | Strict damage constraints, complex biological variability | Rapid screening with minimal preparation | Laboratory | Tumor diagnosis, multimodal fusion, pharmaceutical traceability | [171, 172, 295–312] |
| Hazardous substances detection | Explosives, chemical/biological hazardous materials, and forensic traces | Safety constraints, rapid response | Rapid screening at a safe distance | Field / standoff | Explosive recognition, semi-supervised learning, forensic analysis | [313–316] |
| Cultural heritage analysis | Pigments, mural stratigraphy, and surface composition | Strict damage constraints | Minimally invasive compositional and stratigraphic analysis | On-site | Pigment identification, depth profiling, LIBS–Raman integration | [317–320] |
| Petrological analysis | Elemental composition and lithological information | Mineral heterogeneity, matrix complexity | Rapid analysis of heterogeneous solids | Field / laboratory | Rock classification, portable LIBS, multi-element quantification | [86, 321] |
| Soil monitoring | Heavy metals and soil contaminants | Moisture, heterogeneity | Rapid field screening | In situ / field | Plasma enhancement, portable LIBS, heavy metal quantification | [87, 322–328] |
| Water monitoring | Dissolved elements, nutrients, and contaminants | Low concentration, quenching | Rapid multi-element water-quality sensing | Online / laboratory | Preconcentration, aerosol-assisted LIBS, online monitoring | [329–334] |

# 7 Summary and outlook

Over the past decade, LIBS research in China has advanced significantly in fundamentals, instrumentation, data processing and modeling, and applications. Assessing these advancements within the broader context of global LIBS research helps to better understand their characteristics. Worldwide, the development of LIBS encompasses various paths, including mechanism-centered plasma research [335], mission-level systems such as space exploration [336] and inline industrial instrumentation [337], and other specific application scenarios. In this context, a notable feature of China's LIBS research is the close integration of practical quantitative needs with methodological development, especially in complex real samples. In these fields, research on plasma behavior, instrumentation, data processing, and practical deployment often aims to enhance the quantitative performance of LIBS in real scenarios. In addition to these research and application advancements, a more significant development is the transformation in the understanding of the essential nature of LIBS: namely, that its defining characteristic lies in its signal source, which is a highly transient and spatially inhomogeneous plasma. The three core problems discussed in this review, all centered on this understanding, provide the main framework through which the development of LIBS is interpreted here. Taken together, the progress reviewed here suggests that LIBS is no longer regarded merely as a technique whose optimization is aimed at obtaining stronger emission signals, but rather as an analytical system that must establish a controllable and reliable pathway from a highly dynamic plasma source to reliable analytical results under practical constraints.

The first core problem concerns how to obtain signals with better repeatability and reduced matrix effects. Over the past decade, progress has moved from phenomenological observation toward the clarification of key mechanisms, especially in plasma spatiotemporal evolution, source-side uncertainty generation, surrounding-gas effects and the dependence of signal on the spatiotemporal acquisition window. These advances have made it increasingly clear that the LIBS signal cannot be understood as a direct consequence of experimental parameters alone, but rather as the outcome of a tightly coupled plasma-mediated process. In this context, the introduction of plasma modulation, which directly aims to control plasma evolution, has marked a shift from the paradigm of signal enhancement to that of active plasma regulation, offering a more fundamental route toward obtaining more representative and repeatable observable signals. Nevertheless, this problem remains unresolved in a broader sense: although dominant processes have been identified and some mechanisms have been partially clarified, a unified and predictive description that links plasma formation, evolution, and signal acquisition is still lacking, and many relevant effects remain strongly dependent on specific sample systems, environmental conditions, and measurement configurations. This lack has limited the development of more targeted and mechanism-guided plasma modulation strategies.

The second core problem concerns how to transform raw signals into reliable analytical results. This problem has seen the broadest methodological development. Effective data preprocessing has helped reduce fluctuation-induced uncertainty, while various modeling strategies, including machine learning, physics-based approaches, hybrid models, and multimodal methods, have greatly enhanced the ability of LIBS to cope with signal uncertainty and matrix-related bias. At the same time, however, the ultimate goal of reliable practical analysis has not yet been fully achieved. Physics-based models are limited by simplifying assumptions, while data-driven models are constrained by the quantity and representativeness of training data. Although progress has been made in transfer learn-

ing and domain adaptation, generalization across different instruments, long time spans, and even relatively similar matrices remains a common challenge for data processing and modeling approaches.

The third core problem concerns how to maintain reliable analytical performance under practical constraints. Compared with a decade ago, LIBS in China has made tremendous progress toward practical applications, including the expansion of application scenarios, the design, deployment, and demonstration of integrated platforms for specific tasks, and advances in general-purpose components. As a result, LIBS has moved beyond predominantly laboratory-based demonstrations and entered an active stage of engineering translation. Nevertheless, achieving laboratory-level analytical performance in real-world deployment scenarios remains an unsolved problem. Meeting key deployment requirements, including long-term stability, measurement representativeness, workflow integration, and reliable operation, remains difficult under practical constraints such as limited availability of real-world data and harsh or dynamic environments.

Overall, the three core problems have been answered to markedly different extents. It should be emphasized that these three problems are not independent of one another; rather, they are interconnected and act jointly along the full chain from the understanding and control of the plasma source, to the understanding of raw-signal formation and acquisition, to reliable analytical modeling, and finally to robust deployment in real scenarios. Future progress is likely to depend on several closely related directions. First, with respect to the first core problem, further progress will depend on a deeper understanding of plasma formation, evolution, and signal acquisition through innovative spatiotemporal diagnostic methods and more refined multiphysics simulations. Such understanding is needed to support the development of more effective and mechanism-guided plasma modulation strategies, with the aim of producing a more stable and repeatable plasma. In particular, to better disentangle matrix effects from uncertainty, reducing plasma uncertainty as much as possible should remain the primary task. From this perspective, the uncertainty-reduction effect achieved by plasma modulation may in turn also help disentangle matrix effects from uncertainty and thereby contribute to a better understanding of their respective roles. Second, with respect to the second core problem, data processing and modeling need to move toward more robust, interpretable, and transferable frameworks. Multimodal and hybrid models may be promising directions toward this goal, while transfer learning and domain adaptation also require more integrated progress. Finally, with respect to the third core problem, application-oriented development, in addition to being related to all of the preceding problems, should continue to move toward automation, representative sampling, quality control and automatic feedback, and scenario-specific optimization. In a broader sense, the future of LIBS does not depend on any single technical advance, but on the combined progress of deeper physical understanding, methodological generalization, and engineering implementation.

# Acknowledgements

The authors are grateful for the financial support from the Carbon Neutrality and Energy System Transformation (CNEST) Program led by Tsinghua University and the National Key Research and Development Program of China (No. 2023YFB4102900).

# References


[1] Z. Wang, T. B. Yuan, Z. Y. Hou, W. D. Zhou, J. D. Lu, H. B. Ding, and X. Y. Zeng, Frontiers of Physics **9**, 419 (2014).

[2] J. Yu and R. Zheng, Frontiers of Physics **7**, 647 (2012).

[3] Z. Wang, F. Dong, and W. Zhou, Plasma Science and Technology **17**, 617 (2015).

[4] L.-B. Guo, X.-Y. Li, W. Xiong, X.-Y. Zeng, and Y.-F. Lu, Frontiers of Physics **11**, 1 (2016).

[5] Y. Fu, Z. Hou, Y. Deguchi, and Z. Wang, Plasma Science and Technology **21**, 30101 (2019).

[6] Z. Hou, S. Jeong, Y. Deguchi, and Z. Wang, Plasma Science and Technology **22**, 70101 (2020).

[7] W. Gu, L. Zhang, M. Dong, C. Li, Y. Tian, Z. Hou, Z. Wang, and R. Zheng, Plasma Science and Technology **24**, 80101 (2022).

[8] A. Einstein and L. Infeld, *The Evolution of Physics*, The Growth of Ideas from Early Concepts to Relativity and Quanta (1938).

[9] Z. Wang, M. S. Afgan, W. Gu, Y. Song, Y. Wang, Z. Hou, W. Song, and Z. Li, TrAC Trends in Analytical Chemistry **143**, 116385 (2021).

[10] W. Wang, L. Sun, G. Wang, P. Zhang, L. Qi, L. Zheng, and W. Dong, Journal of Analytical Atomic Spectrometry **35**, 357 (2020).

[11] I. Rodushkin, M. D. Axelsson, D. Malinovsky, and D. C. Baxter, Journal of Analytical Atomic Spectrometry **17**, 1223 (2002).

[12] C. Geertsen, A. Briand, F. Chartier, J.-L. Lacour, P. Mauchien, S. Sjöström, and J.-M. Mermet, Journal of Analytical Atomic Spectrometry **9**, 17 (1994).

[13] M. Chen, T. Yuan, Z. Hou, Z. Wang, and Y. Wang, Spectrochimica Acta Part B-Atomic Spectroscopy **112**, 23 (2015).

[14] Y. Wang, Q. Wang, A. Chen, and M. Jin, Optik **230**, 166338 (2021).

[15] W. Wang, L. Sun, P. Zhang, T. Chen, L. Zheng, and L. Qi, Journal of Analytical Atomic Spectrometry **36**, 1977 (2021).

[16] T. Li, Z. Hou, Y. Fu, J. Yu, W. Gu, and Z. Wang, Analytica Chimica Acta **1058**, 39 (2019).

[17] J. Hou, D. Zhang, Z. Feng, J. Zhu, and L. Zhang, Spectrochimica Acta, Part B: Atomic Spectroscopy **215**, 106925 (2024).

[18] J. Hou, D. Zhang, Z. Feng, J. Zhu, and L. Zhang, Optics Express **31**, 34404 (2023).

[19] B. Xu, P. Yin, J. Hou, J. Tang, and D. Zhang, Optics Express **33**, 12659 (2025).

[20] Z. Hou, W. Gu, T. Li, Z. Wang, L. Li, X. Yu, Y. Zhang, and Z. Liu, Frontiers of Physics **17**, 62503 (2022).

[21] J. Hou, L. Zhang, W. Yin, S. Yao, Y. Zhao, W. Ma, L. Dong, L. Xiao, and S. Jia, Optics Express **25**, 23024 (2017).

[22] J. J. Hou, L. Zhang, Y. Zhao, W. G. Ma, L. Dong, W. B. Yin, L. T. Xiao, and S. T. Jia, Optics Express **27**, 3409 (2019).

[23] R. Yi, L. Guo, C. Li, X. Yang, J. Li, X. Li, X. Zeng, and Y. Lu, Journal of Analytical Atomic Spectrometry **31**, 961 (2016).

[24] J. Wang, Z. Liu, L. Zhu, Z. Song, Y. Zhang, L. Zhang, W. Zhang, G. Wang, Z. Ye, Z. Zhu, W. Yin, and S. Jia, Optics Express **31**, 16423 (2023).

[25] W. Wang, L. Sun, P. Zhang, L. Zheng, and L. Qi, Microchemical Journal **172**, 106964 (2022).

[26] J. Li, Y. Tang, Z. Hao, N. Zhao, X. Yang, H. Yu, L. Guo, X. Li, X. Zeng, and Y. Lu, Journal of Analytical Atomic Spectrometry **32**, 2189 (2017).

[27] F. Rezaei, G. Cristoforetti, E. Tognoni, S. Legnaioli, V. Palleschi, and A. Safi, Spectrochimica Acta Part B: Atomic Spectroscopy **169**, 105878 (2020).

[28] J. Hou, L. Zhang, Y. Zhao, Z. Wang, Y. Zhang, W. Ma, L. Dong, W. Yin, L. Xiao, and S. Jia, Plasma Science and Technology **21**, 34016 (2019).

[29] H. Y. Oderji, N. Farid, L. Sun, C. Fu, and H. Ding, Spectrochimica Acta, Part B: Atomic Spectroscopy **122**, 1 (2016).

[30] C. Fu, D. Wu, Q. Wang, L. Sun, Y. Wang, and H. Ding, Journal of Instrumentation **15** (2), C02022.

[31] S. He, Q. Min, H. Lu, Y. Wu, S. Cao, D. Sun, D. Zhang, M. Su, and C. Dong, Optics Letters **49**, 566 (2024).

[32] J. Cai, M. Dong, Y. Zhang, Y. Chen, Y. Liang, and J. Lu, Spectrochimica Acta, Part B: Atomic Spectroscopy **180**, 106195 (2021).

[33] Z.-Z. Wang, Y. Deguchi, Z.-Z. Zhang, Z. Wang, X.-Y. Zeng, and J.-J. Yan, Frontiers of Physics **11**, 114213 (2016).

[34] Z. Wang, Chemosensors **13**, 5 (2025).

[35] Y. T. Fu, Z. Y. Hou, T. Q. Li, Z. Li, and Z. Wang, Spectrochimica Acta, Part B: Atomic Spectroscopy **155**, 67 (2019).

[36] Y.-T. Fu, W.-L. Gu, Z.-Y. Hou, S. A. Muhammed, T.-Q. Li, Y. Wang, and Z. Wang, Frontiers of Physics **16**, 22502 (2021).

[37] W. Gu, N. Nishi, Z. Hou, Z. Wang, and T. Sakka, Spectrochimica Acta, Part B: Atomic Spectroscopy **206**, 106732 (2023).

[38] P. Zheng, G. Chen, W. Gu, J. Wang, Z. Hou, X. Gao, A. Chen, W. Zhou, L. Guo, Q. Zeng, and Z. Wang, TrAC Trends in Analytical Chemistry **197**, 118709 (2026).

[39] Z. Wang, Z. Hou, S.-l. Lui, D. Jiang, J. Liu, and Z. Li, Optics Express **20**, A1011 (2012).

[40] Y. Fu, Z. Hou, and Z. Wang, Optics Express **24**, 3055 (2016).

[41] J. Jia, H. Fu, H. Wang, Z. Ni, and F. Dong, AIP Advances **9**, 25001 (2019).

[42] H. Chen, M. Dong, J. Cai, Z. Shang, Z. Li, F. Tang, and J. Lu, Journal of Analytical Atomic Spectrometry **38**, 1224 (2023).

[43] Y. Qiu, J. Li, B. Lu, J. Wu, X. Guo, Y. Hang, Y. Li, and X. Li, Journal of Analytical Atomic Spectrometry **39**, 3048 (2024).

[44] Z. Hou, M. S. Afgan, S. Sheta, J. Liu, and Z. Wang, Journal of Analytical Atomic Spectrometry **35**, 1671 (2020).

[45] A. Li, S. Chai, H. Peng, Z. Zhao, J. Ren, and W. Wu, Analytical Chemistry **97**, 3253 (2025).

[46] Z. A. Arp, D. A. Cremers, R. D. Harris, D. M. Oschwald, G. R. Parker, and D. M. Wayne, Spectrochimica Acta Part B-Atomic Spectroscopy **59**, 987 (2004).

[47] J. S. Cowpe, R. D. Pilkington, J. S. Astin, and A. E. Hill, Journal of Physics D-Applied Physics **42**, 165202 (2009).

[48] K. Zhang, W. Song, Z. Hou, and Z. Wang, Frontiers of Physics **19**, 42203 (2024).

[49] L. Liu, X. Huang, S. Li, Y. Lu, K. Chen, L. Jiang, J. F. Silvain, and Y. F. Lu, Optics Express **23**, 15047 (2015).

[50] L. Liu, X. Huang, S. Li, Y. Lu, K. Chen, and Y. F. Lu, in *Laser-Based Micro and Nanoprocessing X*, Vol. 9736, edited by U. Klotzbach, K. Washio, and C. B. Arnold (2016) p. 97361S.

[51] M. Ghezelbash, S. J. Mousavi, A. E. Majd, S. M. R. Darbani, H. Saghafifar, and A. Maleki, Optics and Spectroscopy **121**, 174 (2016).

[52] Y. Song, W. Song, L. Li, W. Gu, K. Kou, M. S. Afgan, Z. Hou, Z. Li, and Z. Wang, Optics and Lasers in Engineering **162**, 107433 (2023).

[53] Y. Song, Z. Hou, X. Yu, W. Yao, and Z. Wang, Analytica Chimica Acta **1335**, 343464 (2025).

[54] Y. Song, Z. Hou, C. Yan, W. Song, C. Zhang, and Z. Wang, Analytical Chemistry **97**, 16383 (2025).

[55] M. Rizwan, M. S. Afgan, S. Saleem, K. Kou, Z. Hou, and Z. Wang, Spectrochimica Acta, Part B: Atomic Spectroscopy **227**, 107168 (2025).

[56] Z. Hou, Z. Wang, J. Liu, W. Ni, and Z. Li, Optics Express **21**, 15974 (2013).

[57] L. B. Guo, Z. Q. Hao, M. Shen, W. Xiong, X. N. He, Z. Q. Xie, M. Gao, X. Y. Li, X. Y. Zeng, and Y. F. Lu, Optics Express **21**, 18188 (2013).

[58] X. Su, W. Zhou, and H. Qian, Journal of Analytical Atomic Spectrometry **29**, 2356 (2014).

[59] H. Yin, Z. Hou, T. Yuan, Z. Wang, W. Ni, and Z. Li, Journal of Analytical Atomic Spectrometry **30**, 922 (2015).

[60] J. Jia, H. Fu, Z. Hou, H. Wang, Z. Wang, F. Dong, Z. Ni, and Z. Zhang, Spectrochimica Acta, Part B: Atomic Spectroscopy **163**, 105747 (2020).

[61] J. Ji, W. Song, Z. Hou, L. Li, X. Yu, and Z. Wang, Analytica Chimica Acta **1235**, 340551 (2022).

[62] J. Yu, Z. Hou, Y. Ma, T. Li, Y. Fu, Y. Wang, Z. Li, and Z. Wang, Spectrochimica Acta, Part B: Atomic Spectroscopy **174**, 105992 (2020).

[63] L. B. Guo, W. Hu, B. Y. Zhang, X. N. He, C. M. Li, Y. S. Zhou, Z. X. Cai, X. Y. Zeng, and Y. F. Lu, Optics Express **19**, 14067 (2011).

[64] L. Ping, H. Ran, W. Ding, X. Qingmei, S. Liying, and D. Hongbin, Plasma Science and Technology **17**, 687 (2015).

[65] C. Li, X. Gao, Q. Li, C. Song, and J. Lin, Plasma Science and Technology **17**, 919 (2015).

[66] W. Ding, L. Ping, S. Liying, H. Ran, and D. Hongbin, Plasma Science and Technology **18**, 364 (2016).

[67] Q. Wang, J.-g. Wang, Y.-x. Liang, X.-l. Chen, B. Wu, Z.-b. Ni, and F.-z. Dong, in *2011 International Conference on Optical Instruments and Technology: Optoelectronic Measurement Technology and Systems*, Vol. 8201, edited by X. Dong, X. Bao, P. P. Shum, and T. Liu (2011) p. 82012I.

[68] S. Li, L. Liu, A. Yan, S. Huang, X. Huang, R. Chen, Y. Lu, and K. Chen, Review of Scientific Instruments **88**, 23109 (2017).

[69] D. H. Zhang, X. X. Yuan, M. G. Su, Q. Min, C. Z. Dong, and D. X. Sun, Physics of Plasmas **25**, 63112 (2018).

[70] D. Sun, Y. Ma, Y. Wang, M. Su, Q. Lu, and C. Dong, Analytical Methods **10**, 2595 (2018).

[71] R. Hai, L. Sun, D. Wu, Z. He, H. Sattar, J. Liu, W. Tong, C. Li, C. Feng, and H. Ding, Journal of Analytical Atomic Spectrometry **34**, 1982 (2019).

[72] Y. Tang, J. Li, Z. Hao, S. Tang, Z. Zhu, L. Guo, X. Li, X. Zeng, J. Duan, and Y. Lu, Optics Express **26**, 12121 (2018).

[73] S. Saleem, M. Rizwan, Y. Song, K. Zhang, Z. Hou, and Z. Wang, Frontiers of Physics **20**, 25201 (2025).

[74] S. Saleem, M. Rizwan, Z. Hou, and Z. Wang, Talanta **295**, 128321 (2025).

[75] W. Zhou, K. Li, Q. Shen, Q. Chen, and J. Long, Optics Express **18**, 2573 (2010).

[76] Z. Hou, Z. Wang, J. Liu, W. Ni, and Z. Li, Optics Express **22**, 12909 (2014).

[77] X. Wang, A. Li, X. Xu, Y. He, S. Qiu, X. Ma, and R. Liu, Spectrochimica Acta, Part B: Atomic Spectroscopy **174**, 105996 (2020).

[78] Q.-X. Li, D. Zhang, Y.-F. Jiang, S.-Y. Li, A.-M. Chen, and M.-X. Jin, Chinese Physics B **31**, 85201 (2022).

[79] J. Liu, Z. Hou, T. Li, Y. Fu, and Z. Wang, Journal of Analytical Atomic Spectrometry **35**, 2274 (2020).

[80] W. Ding, S. Xu, Y. Chen, C. Pan, J. Fang, S. Ma, X. Wang, Y. Xia, and Y. Hu, Analytical Chemistry **97**, 28224 (2025).

[81] D. Zhang, Z. Zhang, M. Zhang, Z. Feng, T. Gu, K. Shen, S. Li, J. Hou, and J. Zhu, Optical Engineering **62**, 36102 (2023).

[82] Z. Feng, S. Li, T. Gu, X. Zhou, Z. Zhang, Z. Yang, J. Hou, J. Zhu, and D. Zhang, Molecules **27**, 6438 (2022).

[83] M. Xu, Q. Lin, G. Yang, T. Xu, T. Zhang, X. Wang, S. Wang, F. Bian, and Y. Duan, RSC Advances **5**, 4537 (2015).

[84] G. Yang, Q. Lin, Y. Ding, D. Tian, and Y. Duan, Scientific Reports **5**, 7625 (2015).

[85] F. Zha, G. Niu, Q. Lin, S. Wang, and Y. Duan, Instrumentation Science & Technology **45**, 650 (2017).

[86] M. Zhang, H. Fu, H. Wang, F. Shi, S. Jamali, Z. Ding, B. Wu, and Z. Zhang, Chemosensors **13**, 18 (2025).

[87] Y.-H. Gu, N.-J. Zhao, M.-J. Ma, D.-S. Meng, Y. Yu, Y. Jia, L. Fang, J.-G. Liu, and W.-Q. Liu, Chinese Physics Letters **33**, 85201 (2016).

[88] J. Cai, M. Dong, Y. Zhang, Y. Chen, H. Chen, Y. Liang, W. Li, and J. Lu, Atomic Spectroscopy **42**, 43 (2021).

[89] X. Huaqin, P. Congyuan, and Z. Bing, Talanta **298**, 128804 (2026).

[90] L. Sun, H. Yu, Z. Cong, Y. Xin, Y. Li, and L. Qi, Spectrochimica Acta, Part B: Atomic Spectroscopy **112**, 40 (2015).

[91] Y. Xin, L.-X. Sun, Z.-J. Yang, P. Zeng, Z.-B. Cong, and L.-F. Qi, Frontiers of Physics **11**, 115207 (2016).

[92] Y. Cheng, S. Wang, F. Chen, J. Liang, Y. Zhang, L. Zhang, W. Yin, S. Jia, and L. Xiao, Journal of Biophotonics **17**, e202400332 (2024).

[93] S. Yao, J. Mo, J. Zhao, Y. Li, X. Zhang, W. Lu, and Z. Lu, Applied Spectroscopy **72**, 1225 (2018).

[94] W. Lu, Q. Yang, Z. Yu, X. Zou, H. Qin, G. Chen, W. Ma, J. Zhuo, C. Chen, X. Chen, S. Yao, and J. Lu, Microwave and Optical Technology Letters **66**, e33991 (2024).

[95] Y. Liu, M. Li, Z. An, T. Zhang, J. Liu, Y. Liang, H. Tang, J. Gong, D. Yan, Z. You, and H. Li, Chinese Journal of Analytical Chemistry **52**, 100450 (2024).

[96] S. Yao, Z. Yu, Z. Hou, L. Guo, L. Zhang, H. Ding, Y. Lu, Q. Wang, and Z. Wang, TrAC, Trends in Analytical Chemistry **177**, 117795 (2024).

[97] M. Dong, D. Oropeza, J. Chirinos, J. J. Gonzalez, J. Lu, X. Mao, and R. E. Russo, Spectrochimica Acta, Part B: Atomic Spectroscopy **109**, 44 (2015).

[98] M. Dong, L. Wei, J. J. Gonzalez, D. Oropeza, J. Chirinos, X. Mao, J. Lu, and R. E. Russo, Analytical Chemistry **92**, 7003 (2020).

[99] C. Li, Z. Hao, Z. Zou, R. Zhou, J. Li, L. Guo, X. Li, Y. Lu, and X. Zeng, Optics Express **24**, 7851 (2016).

[100] J. Li, L. Guo, N. Zhao, X. Yang, R. Yi, K. Li, Q. Zeng, X. Li, X. Zeng, and Y. Lu, Talanta **151**, 234 (2016).

[101] R. Yi, J. Li, X. Yang, R. Zhou, H. Yu, Z. Hao, L. Guo, X. Li, X. Zeng, and Y. Lu, Analytical Chemistry **89**, 2334 (2017).

[102] P. Gao, P. Yang, R. Zhou, S. Ma, W. Zhang, Z. Hao, S. Tang, X. Li, and X. Zeng, Applied Optics **57**, 8942 (2018).

[103] J.-j. Guo, Y. Lu, C.-h. Liu, and R.-e. Zheng, Spectroscopy and Spectral Analysis **36**, 259 (2016).

[104] D. Sun, H. Li, G. Zhang, Y. Yin, M. Su, X. Bai, M. Sikorski, and D. Zhang, Heritage Science **12**, 254 (2024).

[105] S. Xie, T. Xu, X. Han, Q. Lin, and Y. Duan, Journal of Analytical Atomic Spectrometry **32**, 629 (2017).

[106] J. Huang, M. Dong, S. Lu, Y. Yu, C. Liu, J. H. Yoo, and J. Lu, Analyst **144**, 3736 (2019).

[107] Z. Shang, M. Dong, W. Lu, J. Cai, K. Bai, F. Tang, Z. Li, S. Yao, and J. Lu, Atomic Spectroscopy **45** (2024).

[108] Y. Lu, L. Liu, Z. Wu, Z. Xu, Z. Zhao, Z. Hao, J. Shi, and X. He, Journal of Analytical Atomic Spectrometry **38**, 2619 (2023).

[109] Z. Zhao, Z. Hao, Y. Lu, Z. Xu, B. Xu, N. Zhang, L. Liu, J. Shi, and X. He, Acta Optica Sinica **44**, 1130002 (2024).

[110] Y. Zhou, L. Sun, Y. Li, Y. Xin, W. Dong, and J. Wang, Journal of Analytical Atomic Spectrometry **39**, 1778 (2024).

[111] J. Liu, W. Song, W. Gu, Z. Hou, K. Kou, and Z. Wang, Analytica Chimica Acta **1251**, 341004 (2023).

[112] J. A. Bolger, Applied Spectroscopy **54**, 181 (2000).

[113] B. Sallé, J. L. Lacour, P. Mauchien, P. Fichet, S. Maurice, and G. Manhès, Spectrochimica Acta Part B-Atomic Spectroscopy **61**, 301 (2006).

[114] P. Zheng, Z. Sun, J. Wang, G. Chen, Z. Yang, and B. Li, Talanta **297**, 128572 (2026).

[115] F. Tang, M. Dong, J. Cai, Z. Li, K. Chen, W. Li, S. Yao, and J. Lu, Journal of Analytical Atomic Spectrometry **39**, 3025 (2024).

[116] Y. Zhou, J. Wu, M. Shi, M. Chen, J. Li, X. Guo, Y. Hang, C. Pei, and X. Li, Applied Physics Letters **126**, 34103 (2025).

[117] Z. Wang, L. Li, L. West, Z. Li, and W. Ni, Spectrochimica Acta Part B-Atomic Spectroscopy **68**, 58 (2012).

[118] L. Li, Z. Wang, T. Yuan, Z. Hou, Z. Li, and W. Ni, Journal of Analytical Atomic Spectrometry **26**, 2274 (2011).

[119] W. Gu, Z. Hou, W. Song, L. Li, X. Yu, J. Liu, Y. Song, M. S. Afgan, Z. Li, Z. Liu, and Z. Wang, Analytica Chimica Acta **1205**, 339752 (2022).

[120] W. Gu, Z. Hou, W. Song, J. Ji, X. Yu, J. Liu, Y. Song, Z. Li, and Z. Wang, Analytica Chimica Acta **1288**, 342167 (2024).

[121] J. Ji, Z. Hou, W. Gu, X. Yu, and Z. Wang, Analytica Chimica Acta **1359**, 344125 (2025).

[122] P. Zhang, L. X. Sun, H. B. Yu, P. Zeng, L. F. Qi, and Y. Xin, Journal of Analytical Atomic Spectrometry **32**, 2371 (2017).

[123] P. Zhang, L. Sun, H. Yu, P. Zeng, L. Qi, and Y. Xin, Analytical Chemistry **90**, 4686 (2018).

[124] P. Zhang, L. Sun, L. Qi, and H. Yu, Measurement **234**, 114827 (2024).

[125] J. Nie, Y. Zeng, X. Niu, D. Zhang, and L. Guo, Journal of Analytical Atomic Spectrometry **38**, 2387 (2023).

[126] D. Zhang, Z. Chen, J. Nie, Y. Chu, and L. Guo, Journal of Analytical Atomic Spectrometry **39**, 2402 (2024).

[127] G. Chen, P. Zheng, J. Wang, B. Li, X. Liu, Z. Yang, Z. Sun, H. Tian, D. Dong, and L. Guo, Journal of Analytical Atomic Spectrometry **39**, 1971 (2024).

[128] Y. Zhang, M. Dong, J. Cai, Y. Chen, H. Chen, C. Liu, J. H. Yoo, and J. Lu, Journal of Analytical Atomic Spectrometry **37**, 139 (2022).

[129] Y. Lyu, W. Song, Z. Hou, and Z. Wang, Plasma Science and Technology **26**, 75509 (2024).

[130] L. Brunnbauer, Z. Gajarska, H. Lohninger, and A. Limbeck, TrAC, Trends in Analytical Chemistry **159**, 116859 (2023).

[131] Z. Hao, K. Liu, Q. Lian, W. Song, Z. Hou, R. Zhang, Q. Wang, C. Sun, X. Li, and Z. Wang, Frontiers of Physics **19**, 62501 (2024).

[132] S. Lu, M. Dong, J. Huang, W. Li, J. Lu, and J. Li, Spectrochimica Acta, Part B: Atomic Spectroscopy **140**, 35 (2018).

[133] Z. Feng, D. Zhang, B. Wang, J. Ding, X. Liu, and J. Zhu, Plasma Science and Technology **22**, 74012 (2020).

[134] D. Zhang, J. Ding, Z. Feng, R. Yang, Y. Yang, S. Yu, B. Xie, and J. Zhu, Spectrochimica Acta, Part B: Atomic Spectroscopy **180**, 106192 (2021).

[135] E. Harefa and W. Zhou, Sensors **22**, 3129 (2022).

[136] J. Chen, Y. Ding, A. Hu, W. Chen, Y. Wang, M. Zhao, and Y. Shu, Optics Express **31**, 41129 (2023).

[137] X. Cui, Q. Wang, Y. Zhao, X. Qiao, and G. Teng, Applied Physics B: Lasers and Optics **125**, 56 (2019).

[138] Q. Wang, X. Cui, G. Teng, Y. Zhao, and K. Wei, Optics & Laser Technology **125**, 106035 (2020).

[139] S. Jamali, H. Fu, M. Zhang, H. Wang, N. M. Shaikh, B. Wu, B. ul ddin Jamali, F. Shi, Z. Ding, Y. Liu, and Z. Zhang, Applied Spectroscopy **79**, 1455 (2025).

[140] S. Jamali, H. Fu, M. Zhang, H. Wang, N. M. Shaikh, B. Wu, F. Shi, Z. Ding, B. ul ddin Jamali, and Z. Zhang, Analytical Letters (2025).

[141] A. Ciucci, M. Corsi, V. Palleschi, S. Rastelli, A. Salvetti, and E. Tognoni, Applied Spectroscopy **53**, 960 (1999).

[142] J. Yang, X. Li, J. Xu, and X. Ma, Applied Spectroscopy **72**, 129 (2018).

[143] G. H. Cavalcanti, D. V. Teixeira, S. Legnaioli, G. Lorenzetti, L. Pardini, and V. Palleschi, Spectrochimica Acta Part B-Atomic Spectroscopy **87**, 51 (2013).

[144] X. Bai, R. Hai, Z. He, X. Wang, D. Wu, C. Li, W. Tong, H. Wu, G. Xu, D. Dong, Z. Hu, and H. Ding, Journal of Analytical Atomic Spectrometry **37**, 289 (2022).

[145] X. Bai, R. Hai, Z. He, X. Wang, J. Mu, H. Wu, C. Li, D. Wu, G. Xu, Z. Hu, F. Ding, and H. Ding, Spectrochimica Acta Part B: Atomic Spectroscopy **206**, 106724 (2023).

[146] X. Bai, R. Hai, Z. Liu, Z. He, Z. Hu, G. Xu, C. Li, D. Wu, and H. Ding, Optics Express **32**, 35915 (2024).

[147] S. Li, R. Li, Y. Chen, and Q. Huang, Optik **270**, 169946 (2022).

[148] Y. F. Li, Y. Q. Chen, S. S. Li, and X. Q. Huang, Optics Express **30**, 34545 (2022).

[149] S. L. Chen, R. H. Li, and Y. Q. Chen, Applied Optics **62**, 4512 (2023).

[150] J. Huang, M. Dong, S. Lu, W. Li, J. Lu, C. Liu, and J. H. Yoo, Journal of Analytical Atomic Spectrometry **33**, 720 (2018).

[151] Y. Jiang, Z. Lu, X. Chen, Z. Yu, H. Qin, J. Chen, J. Lu, and S. Yao, Analytical Methods **13**, 5467 (2021).

[152] X. Li, H. Lu, J. Yang, and F. Chang, Plasma Science and Technology **21**, 34015 (2019).

[153] X. Li, J. Yang, F. Chang, X. Zheng, and X. He, Journal of Analytical Atomic Spectrometry **34**, 1135 (2019).

[154] F. Chang, H. Lu, H. Sun, and J. Yang, Journal of Analytical Atomic Spectrometry **35**, 2639 (2020).

[155] F. Chang, J. Yang, H. Lu, and H. Li, Journal of Analytical Atomic Spectrometry **36**, 1007 (2021).

[156] J. Yang, X. Li, H. Lu, J. Xu, and H. Li, Journal of Analytical Atomic Spectrometry **33**, 1184 (2018).

[157] Y. Ding, Q. Tan, J. Xu, A. Hu, M. Zhao, X. Li, Y. Shu, and X. Liu, Spectrochimica Acta, Part B: Atomic Spectroscopy **228**, 107171 (2025).

[158] M. Dong, Z. Li, J. Cai, W. Lu, X. Chen, K. Bai, S. Yao, and J. Lu, Spectrochimica Acta, Part B: Atomic Spectroscopy **229**, 107198 (2025).

[159] J. Feng, Z. Wang, L. West, Z. Li, and W. Ni, Analytical and Bioanalytical Chemistry **400**, 3261 (2011).

[160] Z. Wang, J. Feng, L. Li, W. Ni, and Z. Li, Journal of Analytical Atomic Spectrometry **26**, 2175 (2011).

[161] J. Feng, Z. Wang, L. Li, Z. Li, and W. Ni, Applied Spectroscopy **67**, 291 (2013).

[162] X. Li, Z. Wang, Y. Fu, Z. Li, and W. Ni, Spectrochimica Acta, Part B: Atomic Spectroscopy **99**, 82 (2014).

[163] Z. Hou, Z. Wang, T. Yuan, J. Liu, Z. Li, and W. Ni, Journal of Analytical Atomic Spectrometry **31**, 722 (2016).

[164] W. Song, Z. Hou, W. Gu, M. S. Afgan, J. Cui, H. Wang, Y. Wang, and Z. Wang, Spectrochimica Acta, Part B: Atomic Spectroscopy **195**, 106490 (2022).

[165] W. Song, M. S. Afgan, Y.-H. Yun, H. Wang, J. Cui, W. Gu, Z. Hou, and Z. Wang, Expert Systems with Applications **205**, 117756 (2022).

[166] W. Song, Z. Hou, W. Gu, H. Wang, J. Cui, Z. Zhou, G. Yan, Q. Ye, Z. Li, and Z. Wang, Fuel **306**, 121667 (2021).

[167] D. Hall and J. Llinas, Proceedings of the IEEE **85**, 6 (1997).

[168] F. Castanedo, Scientific World Journal (2013).

[169] S. M. Azcarate, R. Rios-Reina, J. M. Amigo, and E. C. Goicoechea, Trac-Trends in Analytical Chemistry **143**, 116355 (2021).

[170] H. Qin, Z. Lu, S. Yao, Z. Li, and J. Lu, Journal of Analytical Atomic Spectrometry **34**, 347 (2019).

[171] M. N. Khan, Q. Wang, B. S. Idrees, G. Teng, W. Xiangli, X. Cui, and K. Wei, Lasers in Medical Science **37**, 2489 (2022).

[172] G. Teng, Q. Wang, X. Cui, K. Wei, W. Xiangli, and G. Chen, Journal of Raman Spectroscopy **52**, 805 (2021).

[173] Q. Zhao, Y. Yu, N. Hao, P. Miao, X. Li, C. Liu, and Z. Li, Microchemical Journal **190**, 108670 (2023).

[174] C. Zhang, W. Song, Y. Lyu, Z. Liu, X. Gao, Z. Hou, and Z. Wang, Analytica Chimica Acta **1351**, 343899 (2025).

[175] S. Yao, H. Qin, S. Xu, Z. Yu, Z. Lu, and Z. Wang, Atomic Spectroscopy **43**, 154 (2022).

[176] W. Song, Z. Hou, W. Gu, M. Ma, C. Zhang, J. Song, F. Rao, H. Wang, and Z. Wang, Engineering Applications of Artificial Intelligence **163**, 113082 (2026).

[177] W. Song, G. Duan, L. An, W. Gu, Y. Lv, Z. Hou, H. Wang, and Z. Wang, Sensors and Actuators B: Chemical **459**, 139880 (2026).

[178] E. R. K. Neo, J. S. C. Low, V. Goodship, S. R. Coles, and K. Debattista, Journal of Cleaner Production **415**, 137919 (2023).

[179] L. Zhang, Y. Gong, Y. Li, X. Wang, J. Fan, L. Dong, W. Ma, W. Yin, and S. Jia, Spectrochimica Acta Part B-Atomic Spectroscopy **113**, 167 (2015).

[180] S. Yao, J. Zhao, Z. Wang, Y. Deguchi, Z. Lu, and J. Lu, Spectrochimica Acta Part B: Atomic Spectroscopy **149**, 249 (2018).

[181] Z. Yu, W. Ma, W. Chen, H. Qin, Q. Ma, Z. Lu, and S. Yao, Spectrochimica Acta, Part B: Atomic Spectroscopy **211**, 106840 (2024).

[182] S. Sheta, M. S. Afgan, Z. Hou, S.-C. Yao, L. Zhang, Z. Li, and Z. Wang, Journal of Analytical Atomic Spectrometry **34**, 1047 (2019).

[183] L. Y. Yu, J. D. Lu, W. Chen, G. Wu, K. Shen, and W. Feng, Plasma Science & Technology **7**, 3041 (2005).

[184] S. Yao, J. Xu, X. Dong, B. Zhang, J. Zheng, and J. Lu, Spectrochimica Acta, Part B: Atomic Spectroscopy **110**, 146 (2015).

[185] X. Li, H. Yin, Z. Wang, Y. Fu, Z. Li, and W. Ni, Spectrochimica Acta, Part B: Atomic Spectroscopy **111**, 102 (2015).

[186] J. Cai, M. Dong, H. Chen, Z. Shang, S. Yao, and J. Lu, Atomic Spectroscopy **45** (2024).

[187] Z. Yu, S. Yao, L. Zhang, Z. Lu, Z. S. Lie, and J. Lu, Journal of Analytical Atomic Spectrometry **34**, 172 (2019).

[188] J. Zheng, J. Lu, B. Zhang, M. Dong, S. Yao, W. Lu, and X. Dong, Applied Spectroscopy **68**, 672 (2014).

[189] S. Yao, L. Zhang, K. Yin, K. Bai, J. Xu, Z. Lu, and J. Lu, Journal of Analytical Atomic Spectrometry **33**, 1676 (2018).

[190] S. Yao, Z. Yu, S. Xu, X. Yao, H. Qin, Z. Lu, and J. Lu, Spectrochimica Acta, Part B: Atomic Spectroscopy **175**, 106014 (2021).

[191] Z. Yu, S. Yao, Y. Jiang, W. Chen, S. Xu, H. Qin, Z. Lu, and J. Lu, Journal of Analytical Atomic Spectrometry **36**, 2473 (2021).

[192] W. Li, M. Dong, S. Lu, S. Li, L. Wei, and J. Lu, Analytical Methods **11**, 4471 (2019).

[193] Y. Chen, M. Dong, J. Cai, H. Chen, Z. Shang, and J. Lu, Journal of Analytical Atomic Spectrometry **37**, 1126 (2022).

[194] S. Yao, H. Qin, Q. Wang, Z. Lu, X. Yao, Z. Yu, X. Chen, L. Zhang, and J. Lu, Spectrochimica Acta Part a-Molecular and Biomolecular Spectroscopy **239**, 118492 (2020).

[195] W. Gu, W. Song, G. Yan, Q. Ye, Z. Li, M. S. Afgan, J. Liu, Y. Song, Z. Hou, Z. Wang, and Z. Li, Spectrochimica Acta, Part B: Atomic Spectroscopy **180**, 106212 (2021).

[196] W. Yin, L. Zhang, L. Dong, W. Ma, and S. Jia, Applied Spectroscopy **63**, 865 (2009).

[197] L. Guo, D. Zhang, L. Sun, S. Yao, L. Zhang, Z. Wang, Q. Wang, H. Ding, Y. Lu, Z. Hou, and Z. Wang, Frontiers of Physics **16**, 22500 (2021).

[198] T. E. Jeffries, N. J. G. Pearce, W. T. Perkins, and A. Raith, Analytical Communications **33**, 35 (1996).

[199] I. Lopez-Quintas, V. Pinon, M. P. Mateo, and G. Nicolas, Applied Surface Science **258**, 9432 (2012).

[200] Q. Yang, X. He, D. Ling, Z. Wei, D. Wei, and Q. Zhang, Spectrochimica Acta, Part B: Atomic Spectroscopy **199**, 106599 (2023).

[201] J. Li, Q. Yang, J. Yao, X. He, and F. Wang, Analytica Chimica Acta **1238**, 340613 (2023).

[202] X. He, B. Dong, B. Zhou, J. Liu, and Y. Wang, Journal of Analytical Atomic Spectrometry **39**, 1417 (2024).

[203] X. He, B. Zhou, Y. Yuan, and L. Kong, Spectrochimica Acta, Part B: Atomic Spectroscopy **220**, 107031 (2024).

[204] X. He, J. Hu, X. Peng, J. Song, Y. Yuan, and J. Qu, Analytica Chimica Acta **1330**, 343271 (2024).

[205] X. He, L. Hu, W. Cheng, J. Quan, Y. Wang, and H. Wang, Spectrochimica Acta, Part B: Atomic Spectroscopy **231**, 107242 (2025).

[206] X. He and H. Wang, Microchemical Journal **216**, 114813 (2025).

[207] H. Kong, L. Sun, J. Hu, Y. Xin, and Z. Cong, Plasma Science & Technology **17**, 964 (2015).

[208] P. Zhang, L. X. Sun, H. Y. Kong, H. B. Yu, M. T. Guo, and P. Zeng, in *Aopc 2017: Optical Spectroscopy and Imaging*, Vol. 10461, edited by J. Yu, Z. Wang, W. Hang, B. Zhao, X. Hou, M. Xie, and T. Shimura (2017) p. UNSP 1046107.

[209] S. Palanco, L. M. Cabalín, D. Romero, and J. J. Laserna, Journal of Analytical Atomic Spectrometry **14**, 1883 (1999).

[210] L. Sun, H. Yu, Z. Cong, H. Lu, B. Cao, P. Zeng, W. Dong, and Y. Li, Spectrochimica Acta, Part B: Atomic Spectroscopy **142**, 29 (2018).

[211] Q. Zeng, C. Pan, C. Li, T. Fei, X. Ding, X. Du, and Q. Wang, Spectrochimica Acta Part B-Atomic Spectroscopy **142**, 68 (2018).

[212] Q. Zeng, C. Pan, T. Fei, X. Ding, S. Wang, and Q. Wang, Journal of Applied Spectroscopy **85**, 817 (2018).

[213] T. Chen, L. Sun, H. Yu, L. Qi, D. Shang, and Y. Xie, Applied Optics **61**, D22 (2022).

[214] T. Chen, L. Sun, H. Yu, P. Zeng, and L. Qi, Spectrochimica Acta, Part B: Atomic Spectroscopy **210**, 106821 (2023).

[215] T. Chen, L. Sun, H. Yu, L. Qi, P. Zhang, and H. Dong, Analyst **149**, 4407 (2024).

[216] T. Yu, H.-x. Yu, P. Zhang, L.-x. Sun, and T. Chen, Spectroscopy and Spectral Analysis **45**, 1334 (2025).

[217] P. Zhang, T. Yu, L. Sun, H. Yu, L. Qi, and L. Zheng, Minerals Engineering **234**, 109715 (2025).

[218] G. Yang, X. Han, C. Wang, Y. Ding, K. Liu, D. Tian, and L. Yao, Analytical Methods **9**, 5365 (2017).

[219] Y. Ding, F. Yan, G. Yang, H. Chen, and Z. Song, Analytical Methods **10**, 1074 (2018).

[220] X. Deng, G. Yang, H. Zhang, and G. Chen, Applied Optics **59**, 2042 (2020).

[221] W. Wang, L. Sun, P. Zhang, L. Zheng, L. Qi, and W. Dong, Plasma Science and Technology **21**, 34004 (2018).

[222] W. Wang, L. Sun, P. Zhang, L. Qi, L. Zheng, and W. Dong, Microchemical Journal **158**, 105267 (2020).

[223] W. Wang, L. Sun, P. Zhang, L. Zheng, L. Qi, and J. Wang, Plasma Science and Technology **23**, 105503 (2021).

[224] S. Li, Z. Qin, J. Lin, L. Ren, Y. Lu, Z. Wang, R. Zheng, and Y. Deguchi, Spectrochimica Acta Part B-Atomic Spectroscopy **234**, 107340 (2025).

[225] Z. Deng, Z. Hao, L. Liu, Z. Xu, Z. Zhao, Y. Lu, J. Shi, and X. He, Journal of Laser Applications **35**, 22003 (2023).

[226] J. Ji, Z. Hou, W. Song, X. Yu, and Z. Wang, Journal of Analytical Atomic Spectrometry **39**, 1885 (2024).

[227] J. Ji, W. Song, Z. Hou, X. Yu, Z. Xing, X. Shen, and Z. Wang, Talanta **305**, 129598 (2026).

[228] B. Thornton, T. Takahashi, T. Sato, T. Sakka, A. Tamura, A. Matsumoto, T. Nozaki, T. Ohki, and K. Ohki, Deep Sea Research Part I: Oceanographic Research Papers **95**, 20 (2015).

[229] T. Takahashi, S. Yoshino, Y. Takaya, T. Nozaki, K. Ohki, T. Ohki, T. Sakka, and B. Thornton, Deep Sea Research Part I: Oceanographic Research Papers **158**, 103232 (2020).

[230] J. Guo, Y. Lu, K. Cheng, J. Song, W. Ye, N. Li, and R. Zheng, Applied Optics **56**, 8196 (2017).

[231] C. Liu, J. Guo, Y. Tian, C. Zhang, K. Cheng, W. Ye, and R. Zheng, Sensors **20**, 7341 (2020).

[232] W. Ye, J. Guo, N. Li, F. Qi, K. Cheng, and R. Zheng, Applied Spectroscopy **74**, 563 (2020).

[233] M. Yu, L. Ren, Y. Tian, Z. Liu, Z. Jia, Y. Xue, P. Chu, W. Ye, C. Li, Y. Lu, J. Guo, and R. Zheng, Analytica Chimica Acta **1345**, 343754 (2025).

[234] M. Sui, Y. Xue, Z. Zhang, Y. Qin, K. Pan, Y. Wang, S. Zhong, and J. Guo, Spectrochimica Acta, Part B: Atomic Spectroscopy **213**, 106875 (2024).

[235] M. Sui, B. Zhao, Z. Jia, Y. Xue, Q. Liu, M. Li, Y. Tian, Y. Lu, X. Zhang, and J. Guo, Spectrochimica Acta, Part B: Atomic Spectroscopy **230**, 107234 (2025).

[236] Y. Tian, S. Hou, L. Wang, X. Duan, B. Xue, Y. Lu, J. Guo, and Y. Li, Analytical Chemistry **91**, 13970 (2019).

[237] Z. Jia, D. Li, Y. Tian, H. Pan, Q. Zhong, Z. Yao, Y. Lu, J. Guo, and R. Zheng, Spectrochimica Acta, Part B: Atomic Spectroscopy **206**, 106713 (2023).

[238] Y. Tian, B. Xue, J. Song, Y. Lu, and R. Zheng, Applied Physics Letters **107**, 111107 (2015).

[239] Z. Jia, Y. Tian, H. Pan, T. Li, Y. Li, Q. Zhong, Z. Yao, Y. Lu, J. Guo, W. Ye, and R. Zheng, Spectrochimica Acta, Part B: Atomic Spectroscopy **209**, 106793 (2023).

[240] Y. Tian, Y. Li, L. Wang, F. Huang, Y. Lu, J. Guo, and R. Zheng, Optics Express **28**, 18122 (2020).

[241] L. Wang, Y. Tian, Y. Li, Y. Lu, J. Guo, W. Ye, and R. Zheng, Plasma Science and Technology **22**, 74004 (2020).

[242] D. Li, Z. Jia, Y. Tian, Y. Li, Y. Lu, W. Ye, J. Guo, and R. Zheng, Optics Express **29**, 44105 (2021).

[243] Y. Tian, H. Pan, C. Zhai, Z. Jia, Q. Zhong, Z. Yao, S. Hou, Y. Lu, J. Guo, and R. Zheng, Plasma Sources Science and Technology **34**, 25012 (2025).

[244] B. Xue, Y. Tian, Y. Lu, Y. Li, and R. Zheng, Spectrochimica Acta, Part B: Atomic Spectroscopy **151**, 20 (2019).

[245] B. Xue, Y. Tian, N. Li, Q. Li, Y. Lu, and R. Zheng, Journal of Analytical Atomic Spectrometry **35**, 2881 (2020).

[246] J. Song, N. Li, Y. Tian, J. Guo, and R. Zheng, Journal of Analytical Atomic Spectrometry **35**, 2351 (2020).

[247] N. Li, N. Nishi, R. Zheng, and T. Sakka, Journal of Analytical Atomic Spectrometry **36**, 1170 (2021).

[248] C. Zhai, Y. Tian, L. Wang, Z. Jia, Y. Li, Y. Lu, J. Guo, W. Ye, and R. Zheng, Journal of Analytical Atomic Spectrometry **39**, 99 (2024).

[249] Y. Tian, L. Wang, B. Xue, Q. Chen, and Y. Li, Journal of Analytical Atomic Spectrometry **34**, 118 (2019).

[250] Y. Tian, B. Xue, J. Song, Y. Lu, and R. Zheng, Applied Physics Letters **109**, 61104 (2016).

[251] L. Wang, Y. Tian, Y. Xue, Z. Jia, C. Zhai, Y. Lu, J. Guo, and R. Zheng, Journal of Analytical Atomic Spectrometry **40**, 1203 (2025).

[252] F. Huang, Y. Tian, Y. Li, W. Ye, Y. Lu, J. Guo, and R. Zheng, Applied Optics **60**, 1595 (2021).

[253] G. Wang, Y. Zeng, L. Guo, S. Li, and Z. Hu, Journal of Analytical Atomic Spectrometry **38**, 2625 (2023).

[254] W. T. Li, Y. N. Zhu, X. Li, Z. Q. Hao, L. B. Guo, X. Y. Li, X. Y. Zeng, and Y. F. Lu, Journal of Analytical Atomic Spectrometry **35**, 1486 (2020).

[255] G. Lu, L. Sun, Z. Cong, and T. Chen, Talanta **270**, 125531 (2024).

[256] G. Lu, L. Sun, Z. Cong, P. Zhang, Y. Li, W. Dong, and J. Wang, Journal of Analytical Atomic Spectrometry **40**, 3485 (2025).

[257] H. Sun, Y. Zhou, J. Li, X. Guo, M. Shi, Z. Hu, J. Wu, X. Li, and J. Li, Talanta **289**, 127706 (2025).

[258] C. Li, C.-L. Feng, H. Y. Oderji, G.-N. Luo, and H.-B. Ding, Frontiers of Physics **11**, 114214 (2016).

[259] C. Li, L. Sun, Z. Hu, D. Zhao, J. Liu, N. Gierse, D. Nicolai, D. Wu, R. Hai, F. Ding, G.-N. Luo, S. Brezinsek, C. Linsmeier, Y. Liang, H. Ding, and the EAST team, Physica Scripta **T171** (2020).

[260] P. Liu, D. Y. Zhao, L. Y. Sun, C. L. Fu, J. M. Liu, C. Li, R. Hai, C. F. Sang, Z. H. Hu, Z. Sun, J. S. Hu, L. Wang, J. L. Chen, Y. F. Liang, G. N. Luo, and H. Ding, Plasma Physics and Controlled Fusion **60**, 85019 (2018).

[261] Z. Hu, N. Gierse, C. Li, J. Oelmann, D. Zhao, M. Tokar, X. Jiang, D. Nicolai, J. Wu, F. Ding, S. Brezinsek, H. Ding, G.-N. Luo, and C. Linsmeier, Fusion Engineering and Design **135**, 95 (2018).

[262] R. Hai, P. Liu, D. Wu, H. Ding, J. Wu, and G.-N. Luo, Fusion Engineering and Design **89**, 2435 (2014).

[263] C. Li, D. Zhao, Z. Hu, X. Wu, G.-N. Luo, J. Hu, and H. Ding, Journal of Nuclear Materials **463**, 915 (2015).

[264] M. Imran, R. Hai, L.-Y. Sun, H. Sattar, Z.-L. He, D. Wu, C. Li, W.-J. Wang, Z.-H. Hu, G.-N. Luo, and H. Ding, Journal of Nuclear Materials **526**, 151775 (2019).

[265] Z. Hu, X. Bai, H. Wu, R. Hai, F. Ding, M. Imran, C. Li, H. Ding, and G.-N. Luo, Nuclear Materials and Energy **41**, 101785 (2024).

[266] Z. Hu, F. Ding, M. Imran, G.-N. Luo, C. Li, R. Hai, and H. Ding, Nuclear Materials and Energy **37**, 101542 (2023).

[267] J. Liu, D. Wu, D. Zhao, S. Liu, X. Hu, C. Li, L. Cai, and H. Ding, Fusion Engineering and Design **195**, 113930 (2023).

[268] C. Li, J. Oelmann, S. Brezinsek, M. Rasinski, C. P. Dhard, R. König, Y. Liang, H. Ding, and C. Linsmeier, Spectrochimica Acta Part B: Atomic Spectroscopy **160**, 105689 (2019).

[269] C. Li, N. Gierse, J. Oelmann, S. Brezinsek, M. Rasinski, C. Prakash Dhard, T. Sunn Pedersen, R. König, Y. Liang, H. Ding, C. Linsmeier, and the W7-X Team, Physica Scripta **2017**, 14004 (2017).

[270] L. Sun, D. Wu, C. Li, J. Wu, S.-H. Hong, E. Bang, Z. Hu, F. Ding, G. Luo, and H. Ding, Nuclear Materials and Energy **31**, 101174 (2022).

[271] Z. He, D. Wu, Y. Lyu, X. Hu, X. Bai, H. Wu, R. Hai, C. Li, and H. Ding, Nuclear Fusion **65**, 106018 (2025).

[272] M. Dong, L. Wei, J. Lu, W. Li, S. Lu, S. Li, C. Liu, and J. H. Yoo, Journal of Analytical Atomic Spectrometry **34**, 480 (2019).

[273] W. Li, J. Lu, M. Dong, S. Lu, J. Yu, S. Li, J. Huang, and J. Liu, Energy & Fuels **32**, 24 (2018).

[274] W. Ma, Z. Yu, Z. Lu, Q. Ma, and S. Yao, Atomic Spectroscopy **44**, 160 (2023).

[275] G. Pan, J. Lu, M. Dong, S. Yao, Z. Xie, and J. Fan, Plasma Science and Technology **17**, 625 (2015).

[276] G. Pan, M. Dong, J. Yu, and J. Lu, Spectrochimica Acta Part B-Atomic Spectroscopy **131**, 26 (2017).

[277] S. Yao, L. Zhang, J. Xu, Z. Yu, and Z. Lu, Energy & Fuels **31**, 12093 (2017).

[278] Y. Zhang, M. Dong, L. Cheng, L. Wei, J. Cai, and J. Lu, Journal of Analytical Atomic Spectrometry **35**, 810 (2020).

[279] H.-b. Fu, B. Wu, H.-d. Wang, M.-y. Zhang, and Z.-r. Zhang, Spectroscopy and Spectral Analysis **42**, 3489 (2022).

[280] D. Qu, G. Yang, X. Jin, G. Chen, Z. Bai, C. Li, and D. Tian, Spectrochimica Acta, Part B: Atomic Spectroscopy **209**, 106794 (2023).

[281] D. Qu, Z. Zhang, J. Liang, H. Liao, and G. Yang, Spectroscopy and Spectral Analysis **44**, 3222 (2024).

[282] Q. Li, Y. Tian, B. Xue, N. Li, W. Ye, Y. Lu, and R. Zheng, Journal of Analytical Atomic Spectrometry **35**, 366 (2020).

[283] B. Wang, W. Song, Y. Tian, Y. Lu, Y. Li, J. Guo, W. Ye, and R. Zheng, Journal of Analytical Atomic Spectrometry **38**, 281 (2023).

[284] R. Hai, X. Wu, Y. Xin, P. Liu, D. Wu, H. Ding, Y. Zhou, L. Cai, and L. Yan, Journal of Nuclear Materials **447**, 9 (2014).

[285] Y. Qiu, J. Wu, X. Li, T. Liu, F. Xue, Z. Yang, Z. Zhang, and H. Yu, Spectrochimica Acta, Part B: Atomic Spectroscopy **149**, 48 (2018).

[286] Y. Chen, Q. Zhang, Y. Zhangcheng, Y. Liu, Z. Zhuo, and L. Li, Optics & Laser Technology **145**, 107490 (2022).

[287] X. Lu, Y. Liu, Q. Zhang, Y. Chen, and J. Yao, Optics & Laser Technology **149**, 107826 (2022).

[288] Z. Sun, J. Feng, W. Gao, Y. Ye, and Y. Liu, Journal of Analytical Atomic Spectrometry **40**, 2327 (2025).

[289] Z. Wang, N. Aizezi, Y. Ye, H. Meng, and Y. Liu, Spectrochimica Acta, Part B: Atomic Spectroscopy **232**, 107270 (2025).

[290] M. Yang, W. Yu, Q. Zhang, Z. Zhou, and Y. Liu, Spectrochimica Acta, Part B: Atomic Spectroscopy **197**, 106541 (2022).

[291] Z. Zhou, Y. Ge, X. Zhang, Y. Ye, M. Yang, Z. Sun, and Y. Liu, Spectrochimica Acta, Part B: Atomic Spectroscopy **220**, 107018 (2024).

[292] C. Li, Z. Lu, J. Chen, Z. Yu, Q. Yang, H. Qin, X. Xing, Q. Ma, and S. Yao, Analytica Chimica Acta **1337**, 343568 (2025).

[293] Z. Lu, X. Chen, S. Yao, H. Qin, L. Zhang, X. Yao, Z. Yu, and J. Lu, Fuel **258**, 116150 (2019).

[294] Z. Lu, X. Chen, Y. Jiang, X. Li, J. Chen, Y. Li, W. Lu, J. Lu, and S. Yao, Renewable Energy **164**, 1204 (2021).

[295] Y. Du, Q. Wang, Y. Zhao, X. Cui, and Z. Peng, Laser Physics **29**, 95602 (2019).

[296] B. S. Idrees, Q. Wang, M. N. Khan, G. Teng, X. Cui, W. Xiangli, and K. Wei, Biomedical Optics Express **13**, 26 (2022).

[297] B. S. Idrees, G. Teng, A. Israr, H. Zaib, Y. Jamil, M. Bilal, S. Bashir, M. N. Khan, and Q. Wang, Biomedical Optics Express **14**, 2492 (2023).

[298] M. N. Khan, Q. Wang, B. S. Idrees, G. Teng, X. Cui, and K. Wei, Journal of Spectroscopy **2020**, 8826243 (2020).

[299] M. N. Khan, Q. Wang, B. S. Idrees, W. Xiangli, G. Teng, X. Cui, Z. Zhao, K. Wei, and M. Abrar, Frontiers in Physics **10**, 821057 (2022).

[300] M. N. Khan, Q. Wang, B. S. Idrees, R. Waheed, A. Ul Haq, M. Abrar, and Y. Jamil, Lasers in Medical Science **38**, 149 (2023).

[301] G. Teng, Q. Wang, H. Yang, X. Qi, H. Zhang, X. Cui, B. S. Idrees, W. Xiangli, K. Wei, and M. N. Khan, Biomedical Optics Express **11**, 4276 (2020).

[302] G. Teng, Q. Wang, H. Zhang, W. Xiangli, H. Yang, X. Qi, X. Cui, B. S. Idrees, K. Wei, and M. N. Khan, Spectrochimica Acta, Part B: Atomic Spectroscopy **165**, 105787 (2020).

[303] G. Teng, Q. Wang, X. Cui, G. Chen, K. Wei, X. Xu, B. S. Idrees, and M. N. Khan, Biomedical Optics Express **12**, 4438 (2021).

[304] Q. Wang, W. Xiangli, G. Teng, X. Cui, and K. Wei, Applied Spectroscopy Reviews **56**, 221 (2021).

[305] Q. Wang, W. Xiangli, X. Chen, J. Zhang, G. Teng, X. Cui, B. S. Idrees, and K. Wei, Biomedical Optics Express **12**, 1999 (2021).

[306] L. Wang, G. Teng, X. Xu, H. Yang, Z. Zhao, B. Lu, H. Zhou, S. Xu, Y. Liu, X. Cheng, J. Huang, H. Yang, and Q. Wang, Spectrochimica Acta, Part B: Atomic Spectroscopy **232**, 107278 (2025).

[307] K. Wei, X. Cui, G. Teng, M. N. Khan, and Q. Wang, Plasma Science and Technology **23**, 85507 (2021).

[308] K. Wei, Q. Wang, G. Teng, X. Xu, Z. Zhao, and G. Chen, Applied Sciences-Basel **12**, 4981 (2022).

[309] K. Wei, G. Teng, Q. Wang, X. Xu, Z. Zhao, H. Liu, M. Bao, Y. Zheng, T. Luo, and B. Lu, Foods **12**, 1710 (2023).

[310] Z. Zhao, W. Ma, G. Teng, X. Xu, K. Wei, G. Chen, Q. Wang, and W. Xu, Spectrochimica Acta, Part B: Atomic Spectroscopy **202**, 106644 (2023).

[311] Z. Zhao, X. Xu, M. Bao, Y. Zheng, T. Luo, B. Lu, G. Teng, Q. Wang, M. N. Khan, and J. Yong, Microchemical Journal **203**, 110955 (2024).

[312] Z. Zhao, W. Xu, G. Teng, X. Xu, B. Lu, H. Zhou, L. Wang, Y. Liu, S. Xu, Q. Wang, and W. Ma, Analytica Chimica Acta **1353**, 343948 (2025).

[313] Q. Wang, G. Teng, Y. Zhao, X. Cui, and K. Wei, IEEE Photonics Journal **11**, 5700212 (2019).

[314] Q. Wang, G. Teng, C. Li, Y. Zhao, and Z. Peng, Journal of Hazardous Materials **369**, 423 (2019).

[315] Y. Zhao, Q. Wang, X. Cui, G. Teng, K. Wei, and H. Liu, Applied Optics **59**, 1329 (2020).

[316] Y. Zhao, Q. Q. Wang, X. Cui, G. Teng, K. Wei, and H. Liu, Frontiers in Physics **9**, 675135 (2021).

[317] W. Han, M. Su, D. Sun, Y. Yin, Y. Wang, C. Gao, F. Yang, and Y. Fu, Plasma Science and Technology **22**, 85501 (2020).

[318] D. Sun, X. Li, Y. Yin, Y. Zhang, W. Han, Y. Wang, M. Su, C. Dong, Z. Yu, and B. Su, Journal of Cultural Heritage **55**, 399 (2022).

[319] Y. Yin, Z. Yu, D. Sun, Z. Shan, Q. Cui, Y. Zhang, Y. Feng, B. Shui, Z. Wang, Z. Yin, B. Chai, W. Zhang, C. Dong, and B. Su, Frontiers in Physics **10**, 847036 (2022).

[320] Y. Zhang, D. Sun, Y. Yin, Z. Yu, B. Su, C. Dong, and M. Su, Plasma Science and Technology **24**, 84003 (2022).

[321] M. Shi, J. Wu, J. Li, D. Wu, N. Wang, Y. Chen, X. Guo, Y. Qiu, Y. Zhou, and A. Qiu, Spectrochimica Acta, Part B: Atomic Spectroscopy **216**, 106933 (2024).

[322] Y.-h. Gu, N.-j. Zhao, M.-j. Ma, D.-s. Meng, Y. Jia, L. Fang, J.-g. Liu, and W.-q. Liu, Spectroscopy and Spectral Analysis **38**, 982 (2018).

[323] E. Harefa, N. Li, and W. Zhou, Journal of Analytical Atomic Spectrometry **37**, 1340 (2022).

[324] L. I. Kexue, W. Zhou, Q. Shen, J. Shao, and H. Qian, Spectrochimica Acta, Part B: Atomic Spectroscopy **65**, 420 (2010).

[325] K. Li, W. Zhou, Q. Shen, Z. Ren, and B. Peng, Journal of Analytical Atomic Spectrometry **25**, 1475 (2010).

[326] M. Ma, L. Fang, N. Zhao, and X. Ma, Chemosensors **12**, 40 (2024).

[327] D. Meng, N. Zhao, M. Ma, L. Fang, Y. Gu, Y. Jia, J. Liu, and W. Liu, Applied Optics **56**, 5204 (2017).

[328] N. J. Zhao, D. S. Meng, Y. Jia, M. J. Ma, L. Fang, J. G. Liu, and W. Q. Liu, Optics Express **27**, A495 (2019).

[329] X. Yang, X. Wang, X. Wang, B. Wang, D. Li, X. Zhang, H. Ren, H. Qin, Z. Zhou, and X. Zheng, Optics Express **31**, 40345 (2023).

[330] X. Yang, X. Wang, D. Li, X. Zhang, K. Li, H. Ren, Z. Zhou, Z. Qin, and X. Zheng, Journal of Analytical Atomic Spectrometry **39**, 433 (2024).

[331] X. Yang, P. Zhu, D. Li, C. Liu, X. Zhang, T. Hong, H. Ren, Z. Hua, Z. Qin, Z. Sun, and X. Zheng, Journal of Analytical Atomic Spectrometry **40**, 498 (2025).

[332] D. C. Zhang, Z. Q. Hu, Y. B. Su, B. Hai, X. L. Zhu, J. F. Zhu, and X. Ma, Optics Express **26**, 18794 (2018).

[333] P. Zheng, H. Zhao, J. Wang, R. Liu, N. Ding, X. Mao, and C. Lai, Journal of Analytical Atomic Spectrometry **35**, 3032 (2020).

[334] P. Zheng, N. Ding, J. Wang, H. Zhao, R. Liu, and Y. Yang, Journal of Analytical Atomic Spectrometry **36**, 2631 (2021).

[335] D. W. Hahn and N. Omenetto, Applied Spectroscopy **64**, 335A (2010).

[336] H. Saeidfirozeh, P. Kubelík, V. Laitl, A. Křivková, J. Vrábel, K. Rammelkamp, S. Schröder, I. Gornushkin, E. Képeš, J. Žabka, M. Ferus, P. Pořízka, and J. Kaiser, TrAC Trends in Analytical Chemistry **181**, 117991 (2024).

[337] R. Noll, C. Fricke-Begemann, M. Brunk, S. Connemann, C. Meinhardt, M. Scharun, V. Sturm, J. Makowe, and C. Gehlen, Spectrochimica Acta Part B: Atomic Spectroscopy **93**, 41 (2014).